AWARD NUMBER: W81XWH-14-1-0305

TITLE:
B-Cell Activation and Tolerance Mediated by B-Cell Receptor, Toll-Like Receptor, and Survival Signal Crosstalk in SLE Pathogenesis

PRINCIPAL INVESTIGATOR:
Michael P. Cancro

CONTRACTING ORGANIZATION:
University of Pennsylvania
Philadelphia, PA 19104-6205

REPORT DATE:
September 2017

TYPE OF REPORT:
Annual

PREPARED FOR:
U.S. Army Medical Research and Materiel Command
Fort Detrick, Maryland 21702-5012

REPORT DOCUMENTATION PAGE

Form Approved
OMB No. 0704-0188

1. REPORT DATE	2. REPORT TYPE	3. DATES COVERED
September 2017	Annual	15Aug2016 - 14Aug2017

4. TITLE AND SUBTITLE
B-Cell Activation and Tolerance Mediated by B-Cell Receptor, Toll-Like Receptor, and Survival Signal Crosstalk in SLE Pathogenesis

5a. CONTRACT NUMBER

5b. GRANT NUMBER
W81XWH-14-1-0305

5c. PROGRAM ELEMENT NUMBER

6. AUTHOR(S)
Michael P. Cancro, Jean L. Scholz

E-Mail: cancro@pennmedicine.upenn.edu

5d. PROJECT NUMBER

5e. TASK NUMBER

5f. WORK UNIT NUMBER

7. PERFORMING ORGANIZATION NAME(S) AND ADDRESS(ES)
University of Pennsylvania
3451 Walnut St.
Philadelphia, PA 19104-6205

8. PERFORMING ORGANIZATION REPORT NUMBER

9. SPONSORING / MONITORING AGENCY NAME(S) AND ADDRESS(ES)

U.S. Army Medical Research and Materiel Command
Fort Detrick, Maryland 21702-5012

10. SPONSOR/MONITOR'S ACRONYM(S)

11. SPONSOR/MONITOR'S REPORT NUMBER(S)

12. DISTRIBUTION / AVAILABILITY STATEMENT

Approved for Public Release; Distribution Unlimited

13. SUPPLEMENTARY NOTES

14. ABSTRACT
We previously found that B cell receptor (BCR)-delivered TLR9 agonists initiate a response involving proliferation followed by abrupt cell death; furthermore, responding cells are rescued by survival cytokines. We posited this as a normal immune response-limiting mechanism that, if thwarted, may lead to persistence of self-reactive antibody-secreting cells. In this proposal we seek to characterize the pathways leading to post-proliferative death and rescue, and to determine how different forms of rescue lead to alternative differentiation outcomes. During the first year period we showed that in the context of BCR-delivered TLR9 signals, IL-21 promotes and IL-4 opposes the T-bet+CD11c+ B cell fate. In the current reporting period, we have extended these findings to show that IFN-gamma also promotes the Tbet+ fate, and that B cells with this phenotype are antigen-experienced cells that emerge in both normal responses to viral infections as well as in autoimmune scenarios. We have forwarded a theoretical framework to explain the link between these activation requisites and humoral autoimmunity.

15. SUBJECT TERMS
regulation of B cell responses; TLR7/9 agonists

16. SECURITY CLASSIFICATION OF:			17. LIMITATION OF ABSTRACT	18. NUMBER OF PAGES	19a. NAME OF RESPONSIBLE PERSON
a. REPORT	b. ABSTRACT	c. THIS PAGE			USAMRMC
Unclassified	Unclassified	Unclassified	Unclassified	32	19b. TELEPHONE NUMBER *(include area code)*

Table of Contents

1. INTRODUCTION: This grant is based on our observation that BCR-delivered TLR9 agonists initiate a self-limiting response involving proliferation and differentiation, followed by abrupt cell death, but that B cells can be rescued from death and directed toward effector fates by survival and differentiation mediators. The planned and ongoing studies are thus to investigate the outcomes of this rescue and differentiation in both murine and human cells – with emphasis on how different forms of rescue lead to alternative fates associated with autoimmune disease.

2. KEYWORDS: Tbet-postive B cell, ABC, autoimmunity, SLE

3. ACCOMPLISHMENTS:

Major goals as stated in the approved SOW

Specific Aim 1: Detail the pathways mediating post proliferative death, rescue, and differentiation of each peripheral B cell subset in mice and humans.

> **Major Task 1.1**: Determine characteristics of death and rescue among several additional mouse and human B cell subsets. **Status: completed.**
>
> **Major Task 1.2**: Assess the intracellular pathways that mediate cell death and rescue in each B cell subset following BCR-delivered TLR9 agonists**. Status: completed.**
>
> **Major Task 1.3**: Further characterize the signaling systems involved in post proliferative death and rescue. **Status: in progress.**

Specific Aim 2: Assess how alternative forms of rescue mediate distinct differentiative outcomes.

> **Major Task 2.1**: Assess whether alternative exogenous signals can rescue post-proliferative cell death. **Status: completed.**
>
> **Major Task 2.2**: Determine the signals through which BLyS versus alternative mechanisms rescue cells following BCR-delivered TLR9 agonists. **Status: completed.**
>
> **Major Task 2.3**: Establish whether cells of each B cell subset adopt plasma cell or germinal center programs following different forms of rescue. **Status: completed.**

Specific Aim 3: Determine whether B cells from selected SLE patients are refractory to post-proliferative death mediated by TLR9 agonists, or more responsive to plasmablast or germinal center B cell differentiation in response to rescue signals.

> **Major Task 3.1**: Assess the response of B cells from SLE patients with potential defects in TLR9 signaling**. Status: in progress.**
>
> **Major Task 3.2**: Determine whether B cells from individuals or mouse lines harboring a risk allele are refractory to post-proliferative death mediated by TLR9 agonists**. Status: completed for lupus-prone mouse lines.**

What were the major goals of the project? In summary, the goals of the project were to detail the pathways/phenotypic outcomes mediating post-proliferative death, rescue, and differentiation of each peripheral B cell subset in mice and humans, and to assess how alternative forms of rescue mediate distinct differentiative outcomes.

What was accomplished under these goals? Our progress toward these goals during the current year has culminated in two primary research publications (appended), one collaborative publication (submitted), one in press review, and one dedicated volume with ten collected reviews/commentaries on T-bet+ B cells in Health and Disease (Cellular Immunol, edited by the PI, M Cancro).

The first research paper discussed here is entitled "*A TLR9 dependent checkpoint governs B cell responses to DNA-containing antigens*" (Sindhava/Oropallo et al., The Journal of Clinical Investigation, May 2017 - Appendix 1). This details the molecular pathways mediating post-proliferative death, rescue, and (in part) differentiation of murine peripheral B cell subsets. In addition, data shown in Figure 5 suggest similar mechanisms occur in human peripheral B cells, a necessary prelude to Major Tasks 3.1 and 3.2. Specific findings (accomplishments) are summarized here by Major Task:

> **Major Task 1.1**: **Determine characteristics of death and rescue among several additional mouse and human B cell subsets.** Figure 3 of this paper (appended) shows that the response to the DNA-containing antigen STIC9 is similar for the transitional 1 (TR1), transitional 2/3 (TR2/3), follicular (FO), and marginal zone (MZ) B cell subsets of mice. Post-proliferative death is rescued by BLyS (Fig. 3A), the death mechanism is mitochondrial apoptosis and via a p38 mediated mechanism in all subsets (Fig. 3B). Fig. 5A shows similar responses by circulating mature naïve human B cells (CD27-) to human STIC9 and human BLyS, and also shows it I via a p38-dependent mechanism.

Major Task 1.2: Assess the intracellular pathways that mediate cell death and rescue in each B cell subset following BCR-delivered TLR9 agonists. Figure 1 of this paper shows that the self-limiting B cell response induced by DNA immune complexes is independent of BCR specificity (AM14 vs C57BL/6), occurs 48-60 hours post-stimulation (panels C & D), can be rescued by BLyS (panels A-D & I), and requires TLR9 signaling yet does not reflect significant differences in TLR9 vs. BCR signal strengths (panels E-H).

Major Task 1.3: Further characterize the signaling systems involved in post proliferative death and rescue. Figure 2 of this paper extensively details the death signaling system and chronology of intracellular events for murine B cells. IN toto these data reveal that this mechanism involves p38-mediated cell cycle arrest that subsequently drives mitochondrial depolarization and caspase-9 mediated mitochondrial apoptosis/cell death. Fig. 2A and 2B show that the death is caspase 9 mediated, and not driven by necroptosis or other cell extrinsic mechanisms. Fig 2C shos that consistent with this, it is rescued in BclxL transgenic B cells. Fig 2D shows that among the MAPK pathways known to be associated with these mechanisms, only the p38K is involved, whereas ERK and JNK are not. Fig 2 E, F and G confirm this conclusion by showing that the caspacse 9 cleavage (2E) and mitochondrial depolarization (2F) and that this is blocked by multiple different p38 inhibitors (2G), ruling out off-target inhibitor effects . Figs 2H, I and J show that cell cycle arrest is the initial event, because it is blocked by the p38 inhibitor, but that blocking mitochondrial death with the BclxL transgene, prevents death but does not reverse the cell cycle arrest event (Fig 2K).

Major Task 2.1: **Assess whether alternative exogenous signals can rescue post-proliferative cell death.** Figure 4 of this paper shows that in addition to BLyS, CD40 costimulation and Tfh cytokines IL-21 and IFN-gamma can "rescue" murine B cells. CD40 ligation 48 hours after activation affords only partial rescue (panel B). Figure 5C shows that these relationships are also true for human naïve B cells, since CD40 ligation rescues human B cells stimulated with human STIC9 and that these rescued cells adopt the Tbet+ fate with IFN-gamma signaling.

Major Task 2.2: **Determine the signals through which BLyS versus alternative mechanisms rescue cells following BCR-delivered TLR9 agonists.** Figures 2 and S2 show that BLyS-mediated rescue requires BR3 but not TACI, consistent with a BCLxL-mediated anti-apoptotic signal.

Major Task 2.3: Establish whether cells of each B cell subset adopt plasma cell or germinal center programs following different forms of rescue. Table 1 shows that BLyS rescue allows STIC9-stimulated murine B cells to secrete antibody (a key characteristic of plasma cells). Figure 4 assesses consequences of the various forms of rescue. Briefly, rescue by BLyS alone leads to antibody secretion by STIC9-stimulated murine B cells of all subsets (Table 1, Fig. 4). CD40 costimulation with IL-21 or IFN-gamma leads to survival, expression of the transcription factor T-bet, and isotype class switching – especially to IgG2c -- in vitro. T-bet upregulation occurs in both murine (Fig. 4) and human (Fig. 5) B cells stimulated with STIC9. These are key findings because T-bet-positive B cells are associated with autoimmunity in both species. Mice immunized with amyloid (protein-DNA) complexes yielded reduced germinal center B cells and reduced class switched antibody (Fig. 4) – consistent with our hypothesis of a B cell-intrinsic self-limiting response to DNA-containing antigens, despite partial rescue by CD40 ligation.

Major Task 3.1: Assess the response of B cells from SLE patients with potential defects in TLR9 signaling. Figure 5 shows results for B cells from normal/healthy human donors, a necessary prelude to studies of B cells from SLE patients.

Major Task 3.2: **Determine whether B cells from individuals or mouse lines harboring a risk allele are refractory to post-proliferative death mediated by TLR9 agonists.** Fig. S1 of this paper shows that B cells of lupus-prone mouse strains undergo a similar post-proliferative death response to wild-type and AM-14 mice.

Separate work conducted collaboratively with the Gearhart Lab, referenced in last year's report, was accepted by the Journal of Immunology and published in March 2017 (Appendix 2). These studies assessed the likely origins of T-bet+ B cells (ABCs) and their general properties. Overall they suggest these are a form of memory B cell that emerges from Germinal Center (GC) reactions. These studies inform Major task 2.3.

Major Task 2.3: Establish whether cells of each B cell subset adopt plasma cell or germinal center programs following different forms of rescue. Figure 1 of this paper shows that generation of T-bet-positive B cells requires MHC Class II and the CD40/CD40L axis. These are thus consistent with the notion that cognate help, in the context of appropriate TLR9 containing antigens, can rescue death. Figure 4 further suggests a germinal center origin for a significant proportion of T-bet+ B cells in aged animals. Again, understanding the origin and nature of T-bet+ B cells is important because these cells appear to be key players in autoimmune disease.

The collaborative publication (with the laboratory of Rachel Ettinger) is entitled "*$CD11c^{hi}$ T-bet+ B cells contribute to the pathogenesis of SLE through generation of autoreactive plasma cells.*" This study shows that T-bet+Cd11c+ B cells are associated with SLE, and correlate with disease status. Further, in SLE patients, these cells are enriched for SLE-associated autoreactive specificities. This work is directly relevant to Major Tasks 3.1 and 3.2 but as it is not yet published, specific figures cannot yet be referenced here because the work is presently in submission.

A project extension was granted in August 2017. During the requested extension we will complete analyses of STAT pathways and the phosphoproteomics involved in our recently described TLR9-dependent B cell checkpoint (Sindhava/Orapallo et al, Appendix 1). In addition, we will enlarge the sample sizes of our analyses of B cells from SLE patients, based on recent findings showing that Tbet+ B cell levels correlate with increasing SLEDAI score in SLE patients (Ettinger et al., under review). We feel this extension will yield further valuable information pertinent to both basic mechanisms of tolerance and to potential therapeutic molecular targets.

This extension will also allow us to better address stated goals not met, particularly **Major Task 1.3**: Further characterize the signaling systems involved in post proliferative death and rescue (to complete this task, we would like to analyze STAT pathways) and Major Task 3.1: Assess the response of B cells from SLE patients with potential defects in TLR9 signaling (we hope to enlarge sample sizes of our analyses of B cells from SLE patients).

What opportunities for training and professional development has the project provided? Although training is not a goal of the project per se, during Year 3 these studies helped to serve as a research training vehicle for postdoctoral trainee Arpita Myles. In addition, Research Associate Vishal J. Sindhava and co-first author of the publication in Appendix 1 was partially supported by this project.

How were the results disseminated to communities of interest? The work under this award has contributed to several peer-reviewed research papers and reviews (see Appendices). In addition, key aspects of the work were presented by MP Cancro at four international meetings or invited seminars (Erlangen University, Erlangen Germany; Tongji Medical College, Wuhan PRC; Shanghai Immunology Institute and Pasteur Institute, Shanghai, PRC); and six invited national seminars (U of Miami, FL; Cincinnati Children's Hospital, OH; UAB, Birmingham, AL; Benaroya Research Institute, Seattle WA; USUHS, Bethesda MD; Genomics Institute of the Novartis Research Foundation, La Jolla CA). In addition, results were presented in posters at the AAI 2017 meeting, Washington, DC; FOCIS annual meeting Chicago, IL; PEGS annual meeting, Boston, MA; and the Mid-Winter Conference of Immunologists, Asilomar CA.

What do you plan to do during the next reporting period to accomplish the goals?

During the six-month project extension, we will complete analyses for Major Tasks 1.3, and extend our work to B cells from SLE patients (Major Tasks 3.1 and 3.2).

4. IMPACT:

What was the impact on the development of the principal discipline(s) of the project?

The work supported by this grant has been highly productive, as evidenced by last year's progress report and further publications since then. In particular, the J Clin Invest publication represents a comprehensive assessment of the signals and pathways involved in generating T-bet+ B cells. Moreover, our description of a TLR9-dependent tolerance checkpoint in B cell responses to DNA-containing antigens, as well as their relationship to the Tbet+ B cell subset ('ABC subset') we previously described, have been largely accepted by the community at large and have established avenues of inquiry now being pursued by multiple labs interested in SLE in particular and humoral autoimmunity in general.

What was the impact on other disciplines? Nothing to report.

What was the impact on technology transfer? Nothing to report.

What was the impact on society beyond science and technology? Nothing to report.

5. CHANGES/PROBLEMS: Nothing to report.

6. PRODUCTS

PUBLICATIONS: The following publications resulted in full or in part from this grant support.

1. Sharma S, Fitzgerald KA, **Cancro MP,** Marshak-Rothstein A. Nucleic Acid-Sensing Receptors: Rheostats of Autoimmunity and Autoinflammation. J Immunol. 2015 Oct 15;195(8):3507-12. doi: 10.4049/jimmunol.1500964. Review. PubMed PMID: 26432899; PubMed Central PMCID: PMC4593056.

2. Rubtsova K, Rubtsov AV, **Cancro MP,** Marrack P. Age-Associated B Cells: A T-bet-Dependent Effector with Roles in Protective and Pathogenic Immunity. J Immunol. 2015 Sep 1;195(5):1933-7. doi: 10.4049/jimmunol.1501209. Review. PubMed PMID: 26297793; PubMed Central PMCID: PMC4548292.

3. Nündel K, Green NM, Shaffer AL, Moody KL, Busto P, Eilat D, Miyake K, Oropallo MA, **Cancro MP,** Marshak-Rothstein A. Cell-intrinsic expression of TLR9 in autoreactive B cells constrains BCR/TLR7-dependent responses. J Immunol. 2015 Mar 15;194(6):2504-12. doi: 10.4049/jimmunol.1402425. Epub 2015 Feb 13. PubMed PMID: 25681333; PubMed Central PMCID: PMC4382804.

4. Naradikian MS, Myles A, Beiting DP, Roberts KJ, Dawson L, Herati RS, Bengsch B, Linderman SL, Stelekati E, Spolski R, Wherry EJ, Hunter C, Hensley SE, Leonard WJ, **Cancro MP.** Cutting Edge: IL-4, IL-21, and IFN-g Interact to Govern T-bet and CD11c Expression in TLR-Activated B cells. J Immunol. 2016 Aug 15;197(4):1023-8. doi: 10.4049/jimmunol.1600522. Epub 2016 Jul 18. PMID: 27430719

5. Naradikian MS, Hao Y, **Cancro MP.** Age Associated B cells: Key mediators of both protective and autoreactive humoral responses. Immunol Rev. 2016 Jan;269(1):118-29. doi: 10.1111/imr.12380. PMID: 26683149

6. Russel Knode LM, Naradikian MS, Scholz JL, Hao Y, Liu D, Ford ML, Tobias JW, Ca**ncro MP,** Gearhart PJ. Age-associated B cells express a diverse repertoire of mutated immunoglobulins and share transcriptional profiles with memory cells. J Immunol. 2017 Mar 1;198(5):1921-1927. doi: 10.4049/jimmunol.1601106. Epub 2017 Jan 16. PMID:28093524 **APPENDED**

7. Sindhava VJ, Oropallo MA, Moody K, Naradikian MS, Higdon LE, Zhou L, Myles A, Green N, Nündel K, Stohl W, Schmidt AM, Cao W, Dorta-Estremera S, Kambayashi T, Marshak-Rothstein A, **Cancro MP.** A TLR9-dependent checkpoint governs B cell responses to DNA-containing antigens. J Clin Invest. 2017 May 1;127(5):1651-1663. doi: 10.1172/JCI89931. Epub 2017 Mar 27. PMID:28346226 **APPENDED**

8. Scholz, JL, Sindhava, V, and Cancro MP. The ABCs of a new memory B cell subset. *ASHI Quarterly*. 41***: in press July 2017***

9. Cancro MP Expanding roles for T-bet+ B cells in Immunological health and Disease. *Cellular Immunol* ***in press 2017***

Myles, A and **Cancro, MP*** Signals determining T-bet expression in B cells. *Cellular immunol* ***In Press, 2017***

One additional manuscript based in part on the findings described above is also currently under revision.

10. Wang S, Want J, Naiman B, Karnell J, Gross P, Rahman S., Siegel R, Hasni S, **Cancro MP,** Kolbeck R, Ettinger R. CD11c expression in T-bet+ B cells is driven by IL-21 and associated with autoimmune disease manifestations in SLE. **UNDER REVISION**

Meeting Abstracts

Arpita Myles and Michael P Cancro. "Co-stimulation and cytokines differentially regulate metabolic profiles in activated B cells" Asilomar Midwinter conference of Immunologists. (January 2017, Asilomar CA)

Shu Wang*, Jingya Wang*, Brian Naiman*, Jodi Karnell*, Phil Gross*, Saifur Rahman*, Molecular Medicine Group, Richard Siegel†, Sarfaraz Hasni†, Michael P. Cancro^, Roland Kolbeck* and Rachel Ettinger* "CD11c expression in B cells is driven by IL-21 and associates with autoimmune disease manifestations in SLE." *2017 American Assoc. of Immunologists Annual Meeting (*May 2017 Washington, D.C.)

Patricia J. Gearhart, Lisa M. Russell Knode, Martin S. Naradikian, and Michael P. Cancro. Age-associated B cells express a diverse repertoire of mutated immunoglobulins and share transcriptional profiles with memory cells *NIH Symposium on Immune dysregulation in Aging*. (September 2016, Arlington VA)

Shu Wang, Jingya Wang, Brian Naiman*, Jodi Karnell*, Phil Gross*, Saifur Rahman*, Molecular Medicine Group, Richard Siegel†, Sarfaraz Hasni†, Michael P. Cancro^, Roland Kolbeck* and Rachel Ettinger* Role and regulation of CD11c+Tbet+ B cells in SLE. *FOCIS Annual Meeting* (June 2017, Chicago, IL

Shu Wang, Jingya Wang, Brian Naiman*, Jodi Karnell*, Phil Gross*, Saifur Rahman*, Molecular Medicine Group, Richard Siegel†, Sarfaraz Hasni†, Michael P. Cancro^, Roland Kolbeck* and Rachel Ettinger* Altered B Cell Subsets in SLE. *PEGS annual meeting* (May 2017 Boston MA)

Presentations by MP Cancro

International

- Sep, 2016 "Now we know our ABCs: T-bet driven effectors of protective and autoimmune responses" 5th international GK Symposium on Regulators of Adaptive Immunity, Erlangen, Germany

- Nov, 2016 "Innate, adaptive, and & survival signals: Targets for modulating B cell tolerance & selection" Tongji Medical College, Huazhong University of Science and Technology, Wuhan, Peoples Republic of China
- Dec, 2016 "Now we know our ABCs: Expanding roles for T-bet+ B cells in health and disease" Shanghai Immunology institute, Shanghai, Peoples Republic of China
- Dec, 2016 "Integrating innate, adaptive, & survival signals to control B cell selection, homeostasis and tolerance" Pasteur Institute of Shanghai, Shanghai, Peoples Republic of China

National

- Sep, 2016 "Memory B cell subsets" ASHI 42nd Annual Meeting. Symposium on "Targeting B, Plasma Cells and Complement for the Treatment of Allograft Rejections" St. Louis, MO
- Nov, 2016 "Now we know our ABCs? Expanding roles for T-bet+ B cells in health and disease." Immunology and Microbiology guest seminar series, Univ. of Miami Miller School of Medicine, Miami, FL
- Feb, 2017 "Now we know our ABCs: T-bet driven effectors of protective and autoimmune responses" Genomics Institute of the Novartis Research Foundation, La Jolla, CA
- Apr, 2017 "Now we know our ABC's Tbet driven effectors of protective and autoimmune responses" Immunology Seminar Series; Cincinnati Children's Hospital Medical Center, Cincinnati OH
- May, 2017 "Now we know our ABCs: Expanding roles for T-bet+ B cells in health and disease." Guest Seminar Series, Department of Microbiology and Immunology, University of Alabama Birmingham, Birmingham, AL
- May, 2017 "How to review scientific manuscripts: Forests or trees?" American Association of Immunologists Annual Meeting, Washington, D.C.

Website(s) or other Internet site(s) Nothing to report.

Technologies or techniques Nothing to report.

Inventions, patent applications, and/or licenses Nothing to report.

Other Products Nothing to report.

7. PARTICIPANTS AND COLLABORATING ORGANIZATIONS:

Name	**Michael P. Cancro**
Project Role	**P.I.**
Researcher Identifier	**N/A**
Nearest person month worked	**2**
Contribution to project	**Principal Investigator; oversee all research**
Funding support	**This award; R01-AI-118691 (NIAID)**

Name	**Jean L. Scholz**
Project Role	**Research Associate**
Researcher Identifier	**N/A**
Nearest person month worked	**3**
Contribution to project	**Perform experiments and oversee logistics**
Funding support	**This award; R01-AI-118691 (NIAID)**

Name	**Arpita Myles**
Project Role	**Postdoc**
Researcher Identifier	**N/A**
Nearest person month worked	**4**
Contribution to project	**Perform experiments related to Tbet+ B cells, cell signaling mechanisms**
Funding support	**This award; R01-AI-118691 (NIAID)**

Name	**Vishal J. Sindhava**
Project Role	**Research Associate**
Researcher Identifier	**N/A**
Nearest person month worked	**3**

Contribution to project	**Perform experiments related to Tbet+ B cells, cell cycle / cell signaling**
Funding support	**This award; R01-AI-118691 (NIAID)**

Has there been a change in the active other support of the PD/PI(s) or senior/key personnel since the last reporting period?
No change.

The following grants were received or renewed during the past year:

R01 AI118691-01; Cancro, Michael (PI); 02/10/15-01/31/20
Mechanistic studies of BLyS-mediated modulation in HIV-1 Env-specific antibody responses

T32 AI055428-12; Cancro, Michael (PI); 06/01/03-07/31/19
Training Program in Immune System Development and Regulation

1 R21 AI133998-01 (D. Allman and MP Cancro multi PI); 06/01/2017-05/31/2019
Plasma Cell Priming

What other organizations were involved as partners?
Nothing to report.

8. SPECIAL REPORTING REQUIREMENTS: Does not apply.

9. APPENDICES:

Appendix 1: Sindhava VJ, Oropallo MA, Moody K, Naradikian MS, Higdon LE, Zhou L, Myles A, Green N, Nündel K, Stohl W, Schmidt AM, Cao W, Dorta-Estremera S, Kambayashi T, Marshak-Rothstein A, **Cancro MP.** A TLR9-dependent checkpoint governs B cell responses to DNA-containing antigens. J Clin Invest. 2017 May 1;127(5):1651-1663. doi: 10.1172/JCI89931. Epub 2017 Mar 27. PMID:28346226

Appendix 2: Russel Knode LM, Naradikian MS, Scholz JL, Hao Y, Liu D, Ford ML, Tobias JW, Ca**ncro MP,** Gearhart PJ. Age-associated B cells express a diverse repertoire of mutated immunoglobulins and share transcriptional profiles with memory cells. J Immunol. 2017 Mar 1;198(5):1921-1927. doi: 10.4049/jimmunol.1601106. Epub 2017 Jan 16. PMID:28093524

A TLR9-dependent checkpoint governs B cell responses to DNA-containing antigens

Vishal J. Sindhava,[1] Michael A. Oropallo,[1] Krishna Moody,[2,3] Martin Naradikian,[1] Lauren E. Higdon,[1] Lin Zhou,[1,4] Arpita Myles,[1] Nathaniel Green,[2,3] Kerstin Nündel,[3] William Stohl,[5] Amanda M. Schmidt,[1] Wei Cao,[6] Stephanie Dorta-Estremera,[6] Taku Kambayashi,[1] Ann Marshak-Rothstein,[3] and Michael P. Cancro[1]

[1]Department of Pathology and Laboratory Medicine, University of Pennsylvania, Perelman School of Medicine, Philadelphia, Pennsylvania, USA. [2]Department of Microbiology, Boston University School of Medicine, Boston, Massachusetts, USA. [3]Department of Medicine, University of Massachusetts School of Medicine, Worcester, Massachusetts, USA. [4]Department of Laboratory Medicine, Shanghai Changzheng Hospital, Second Military Medical University, Shanghai, China. [5]Division of Rheumatology, Department of Medicine, University of Southern California Keck School of Medicine, Los Angeles, California, USA. [6]Department of Immunology, University of Texas MD Anderson Cancer Center, Houston, Texas, USA.

Mature B cell pools retain a substantial proportion of polyreactive and self-reactive clonotypes, suggesting that activation checkpoints exist to reduce the initiation of autoreactive B cell responses. Here, we have described a relationship among the B cell receptor (BCR), TLR9, and cytokine signals that regulate B cell responses to DNA-containing antigens. In both mouse and human B cells, BCR ligands that deliver a TLR9 agonist induce an initial proliferative burst that is followed by apoptotic death. The latter mechanism involves p38-dependent G_1 cell-cycle arrest and subsequent intrinsic mitochondrial apoptosis and is shared by all preimmune murine B cell subsets and CD27$^-$ human B cells. Survival or costimulatory signals rescue B cells from this fate, but the outcome varies depending on the signals involved. B lymphocyte stimulator (BLyS) engenders survival and antibody secretion, whereas CD40 costimulation with IL-21 or IFN-γ promotes a T-bet$^+$ B cell phenotype. Finally, in vivo immunization studies revealed that when protein antigens are conjugated with DNA, the humoral immune response is blunted and acquires features associated with T-bet$^+$ B cell differentiation. We propose that this mechanism integrating BCR, TLR9, and cytokine signals provides a peripheral checkpoint for DNA-containing antigens that, if circumvented by survival and differentiative cues, yields B cells with the autoimmune-associated T-bet$^+$ phenotype.

Introduction

Despite the elimination of many autoreactive B cells during development (1, 2), mature B cell pools include a substantial proportion of polyreactive and self-reactive clonotypes (3–5). This observation suggests that later, activation-associated checkpoints exist to minimize the likelihood that such cells will engage in antibody production, memory B cell formation, or affinity maturation focused on self-antigens. Several recent observations bear directly on this possibility. First, mounting evidence indicates that neither the presence nor the activation of these autoreactive clones is sufficient to engender autoantibody production; instead, additional signals are needed to overcome regulatory constraints that prevent frank autoimmunity (6–14). Cognate T cell help, B lymphocyte stimulator (BLyS, also known as BAFF), IFN-γ, and IL-21 have been implicated as possible second signals (15–25). BLyS overexpression yields humoral autoimmunity (13), and both IFN-γ and IL-21 play roles in systemic autoimmune diseases (26–29). Second, many autoantibodies bind DNA- or RNA-containing complexes, and numerous studies link the endosomal nucleic acid–sensing receptors TLR9 and TLR7 to autoimmune diseases (12, 13, 15, 18, 30–34). Surprisingly, TLR9 deficiency exacerbates autoimmune symptoms in several mouse models, indicating that TLR9 may play a role in limiting the activation of autoreactive B cells. Finally, recent evidence ties this signaling triad — B cell receptor (BCR), TLR7/9, and IL-21 or IFN-γ — to the generation of T-bet$^+$CD11c$^+$ B cells (35), which are associated with autoimmunity in both mice and humans (36, 37). Together, these observations suggest a relationship among the BCR, TLR9, and cytokines that govern both normal and self-reactive antibody responses to nucleic acid–containing antigens, but the nature of this tripartite interaction remains unclear.

Herein, we show that in both mouse and human B cells, TLR9 agonists linked to BCR ligands induce apoptotic death after an initial proliferative burst. The underlying mechanism involves p38 MAPK–dependent cell-cycle arrest, followed by intrinsic mitochondrial apoptosis. However, B cells undergoing this program can be rescued, and the mode of rescue determines subsequent B cell fate. Whereas BLyS affords differentiation to antibody secretion, CD40 costimulation with either IFN-γ or IL-21 yields the T-bet$^+$ B cell phenotype. Finally, we show in vivo that when antigens are complexed with DNA, the magnitude and quality of humoral responses are altered. Together, these findings reveal a cell-intrinsic, TLR9-dependent mechanism that governs the initiation, quality, and extent of B cell responses to DNA-associated antigens. Further, our data suggest that breaching this checkpoint may provide a route to autoimmunity in the context of DNA-containing self-antigens.

Authorship note: V.J. Sindhava and M.A. Oropallo contributed equally to this work.
Conflict of interest: The authors have declared that no conflict of interest exists.
Submitted: August 8, 2016; **Accepted:** January 26, 2017.
Reference information: *J Clin Invest*. 2017;127(5):1651–1663.
https://doi.org/10.1172/JCI89931.

Results

DNA immune complexes induce self-limiting B cell responses that are rescued by BLyS. Prior studies showed that rheumatoid factor–transgenic (RF-transgenic) B cells from AM14 mice proliferate in a TLR9-dependent manner when stimulated with chromatin immune complexes (ICs) formed by the monoclonal antibody PL2-3 (38). To reconcile these findings with exacerbated autoimmune disease in *Tlr9*$^{-/-}$ mice, we performed analyses of cell division and survival under varying conditions. In these experiments, we used CD23^{+} splenic B cells, which are 95% or more quiescent follicular (FO) B cells. Either BCR cross-linking with F(ab′)$_2$ fragments of rabbit anti-mouse IgM (anti-μ) or TLR9 stimulation with the oligodeoxynucleotide 1826 (ODN 1826) induced several rounds of division, with the majority of cells remaining alive (Figure 1A). We observed similar results in cells stimulated with a combination of ODN 1826 and anti-μ. In contrast, proliferation induced by PL2-3 ICs was followed by overwhelming cell death (Figure 1A). This did not reflect nutrient exhaustion, since replenishing chromatin-IC–stimulated cultures with fresh medium had no ameliorating effect. Strikingly, BLyS rescued the chromatin-IC–stimulated B cells, restoring viability at all time points (Figure 1, A and C).

To establish whether this response is characteristic of all B cells, regardless of BCR specificity, we synthesized a stimulatory TLR9 immune complex (STIC9) consisting of a biotinylated CpG-rich dsDNA fragment of approximately 600 bp derived from a murine genomic CpG island sequence, termed clone 11 (39), linked to biotinylated Fab fragments of rabbit anti-mouse IgM via streptavidin (SA) (Figure 1B, inset). In contrast to smaller, thioester-linked CpG oligonucleotides like ODN 1826, clone 11 cannot freely enter B cells but is transported to a TLR9 compartment by BCR-mediated internalization. Thus, STIC9 mirrors PL2-3 IC stimulation, but is independent of BCR specificity, involves only TLR9, and eliminates potential Fc-γ receptor engagement.

Splenic CD23^{+} B cells stimulated with STIC9 recapitulated the post-proliferative death and BLyS-mediated rescue seen with PL2-3–stimulated RF B cells (Figure 1B). A CpG-negative dsDNA IC (CGNEG) synthesized in a manner identical to our synthesis of STIC9 mimicked anti-μ alone, reflecting BCR cross-linking without concomitant TLR9 engagement (Figure 1B). We investigated the timing of post-proliferative death to allow the appropriate design of sampling points in subsequent mechanistic studies. The kinetics of post-proliferative death were similar in both PL2-3–stimulated RF-transgenic AM14 or STIC9-stimulated C57BL/6 B cells, commencing by 48 hours after stimulation and being virtually completed by 60 hours (Figure 1, C and D). Importantly, STIC9 and PL2-3 induced similar degrees of post-proliferative death in B cells from AM14 mice, indicating that STIC9 engages the key elements triggered by the natural autoantigen (Supplemental Figure 1A; supplemental material available online with this article; https://doi.org/10.1172/JCI89931DS1). Moreover, B cells from several lupus-prone strains — NZB/W F1, Sle1, Sle2, and Sle3 — showed similar post-proliferative death responses (Supplemental Figure 1, B and C). Thus, the breakthrough of autoantibody production in these models probably reflects inappropriate rescue and differentiation rather than an intrinsic defect in this mechanism per se.

The post-proliferative death response depends on TLR9 signals, since the proliferation and survival of *Tlr9*$^{-/-}$ B cells treated with STIC9 resembled anti-μ–stimulated cells, reflecting BCR cross-linking in the absence of a TLR9 signal, despite internalization of the DNA CpG motif (Figure 1, E and F). Importantly, the death response induced by STIC9 does not reflect substantial differences in BCR or TLR9 signal strengths, as the degrees of spleen-associated tyrosine kinase (SYK) phosphorylation and downstream nerve growth factor IB (Nur77) induction were similar in cultures stimulated with either STIC9 or anti-μ plus ODN 1826 (Figure 1, G and H). Moreover, ODN 1826 directly coupled to anti-μ mimicked STIC9, ruling out the possibility that differences in TLR9 binding valency or receptor avidity were responsible (Figure 1I). Thus, both natural and defined BCR ligands containing TLR9 agonists drive a unique program that abruptly terminates B cell activation and expansion. Further, this self-limiting response is extended by survival-promoting signals like BLyS.

Post-proliferative death involves intrinsic mitochondrial cell death following p38-dependent cell-cycle arrest. We next interrogated the mechanisms of STIC9-induced B cell death. Post-proliferative death did not reflect *trans* effects, since PL2-3 had no effect on the survival of B6.SJL B cells cocultured with PL2-3–stimulated AM14 B cells (data not shown). Instead, we found that STIC9 directly induced apoptotic cell death, as revealed by caspase 9 and caspase 3 cleavage, which was blocked by BLyS (Figure 2A). Since apoptosis involves either a caspase 8–dependent extrinsic pathway or a caspase 8–independent intrinsic pathway, we asked which is initiated by STIC9. Because caspase 8–KO mice are embryonically lethal unless receptor-interacting protein kinase 3 (RIP3) is also absent (40), we compared STIC9-activated B cells from C57BL/6, *RIP3*$^{-/-}$, and caspase 8$^{-/-}$ *RIP3*$^{-/-}$ mice. STIC9 induced equivalent cell death in the double-KO and control cell populations (Figure 2B), implicating the intrinsic apoptotic death pathway and attendant mitochondrial depolarization. BLyS-mediated rescue, as evidenced by blocked caspase 9 and 3 cleavage (Figure 2A), is consistent with death via this pathway, since BLyS sustains mitochondrial stability (41–43). Two BLyS receptors, BLyS receptor 3 (BR3, also known as BAFFR) and transmembrane activator and CAML interactor (TACI), are expressed on mature naive B cells, and either could account for the BLyS-mediated rescue (44, 45). STIC9 stimulation upregulated both BR3 and TACI (Supplemental Figure 2, A and B), but while rescue was intact in *Taci*$^{-/-}$ B cells, BLyS failed to rescue STIC9-stimulated BR3-deficient B cells (Supplemental Figure 2, C and D). Thus, BLyS-mediated rescue of post-proliferative death requires BR3, whereas TACI is dispensable. Consistent with the well-established ability of BR3 to induce BCL-XL and other antiapoptotic BCL-2 family members (43), B cells from BCL-XL–transgenic mice, which overexpress BCL-XL in the B cell lineage, resisted STIC9-mediated cell death, even in the absence of BLyS (Figure 2C). Finally, mitochondrial depolarization following STIC9 stimulation was confirmed by flow cytometric analyses and was prevented by BCL-XL overexpression (Figure 2C).

While these observations showed that intrinsic mitochondrial death is the ultimate route to TLR9-dependent post-proliferative death, the upstream initiating events remained unclear. Three MAPK mediators, the JNK, ERK, and p38 kinases, are integral to both BCR and TLR9 signaling (46, 47). MAPK signaling differs in AM14 B cells stimulated by PL2-3 versus those stimulated by anti-μ or ODN 1826 (48). Moreover, DNA-containing antigens

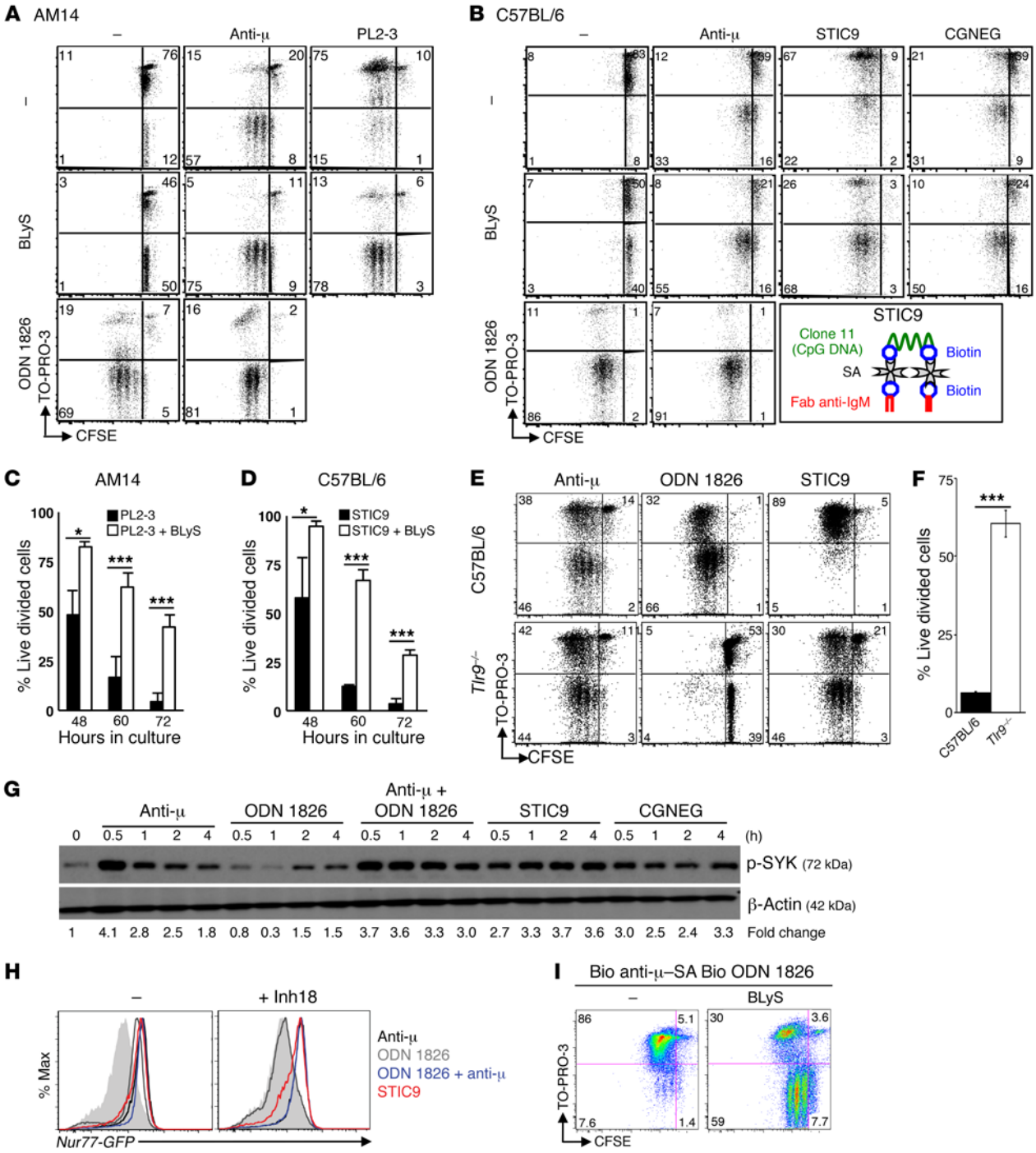

Figure 1. Addition of BLyS prevents AM14 and WT B cells from undergoing proliferation-associated cell death following stimulation with BCR-delivered TLR9 ligands. Representative FACS analysis at 60 hours (**A**) and percentage of live divided cells at 48, 60, and 72 hours (**C**) in AM14 CD23$^+$ splenocytes cultured with the indicated stimuli in the presence or absence of BLyS. Dead cells were stained with TO-PRO-3, while CFSE dilution indicates proliferation. (**B** and **D**) Representative FACS analysis at 60 hours (**B**) and percentage of live divided cells at 48, 60, and 72 hours (**D**) in C57BL/6 CD23$^+$ splenocytes cultured with the indicated stimuli in the presence or absence of BLyS. Diagram in **B** (inset) depicts the structure of STIC9. (**E** and **F**) Representative FACS analysis at 60 hours (**E**) and percentage of live divided cells 60 hours after STIC9 stimulation (**F**) in C57BL/6 and *Tlr9*$^{-/-}$ CD23$^+$ B cells. (**G**) Immunoblot analysis of p-SYK in protein extracts isolated from CD23$^+$ C57BL/6 splenocytes cultured with the indicated stimuli. Fold-change differences in expression are shown compared with unstimulated cells. Values in parentheses indicate the molecular weight. (**H**) FACS analysis of B cells from *Nur77-GFP* reporter mice at 5 hours, cultured with the indicated stimuli, with or without TLR9 inhibitor (Inh18) as described previously (84). Gray-filled area represents no stimulation; black line represents F(ab′)$_2$ fragments of anti-IgM; gray line represents ODN 1826; blue line represents F(ab′)$_2$ fragments of anti-IgM plus ODN 1826; and red line represents STIC9. Max, maximum. (**I**) Representative FACS plots show the proliferation and survival of C57BL/6 CD23$^+$ splenocytes cultured for 60 hours with SA-linked biotinylated (Bio) ODN 1826 and biotinylated F(ab)$_2$, in the presence or absence of BLyS. Data represent a minimum of 3 independent experiments with 3 mice each. Error bars indicate the mean ± SEM. $^*P < 0.05$ and $^{***}P < 0.001$, by 2-tailed Student's *t* test. "–" signifies unstimulated cells.

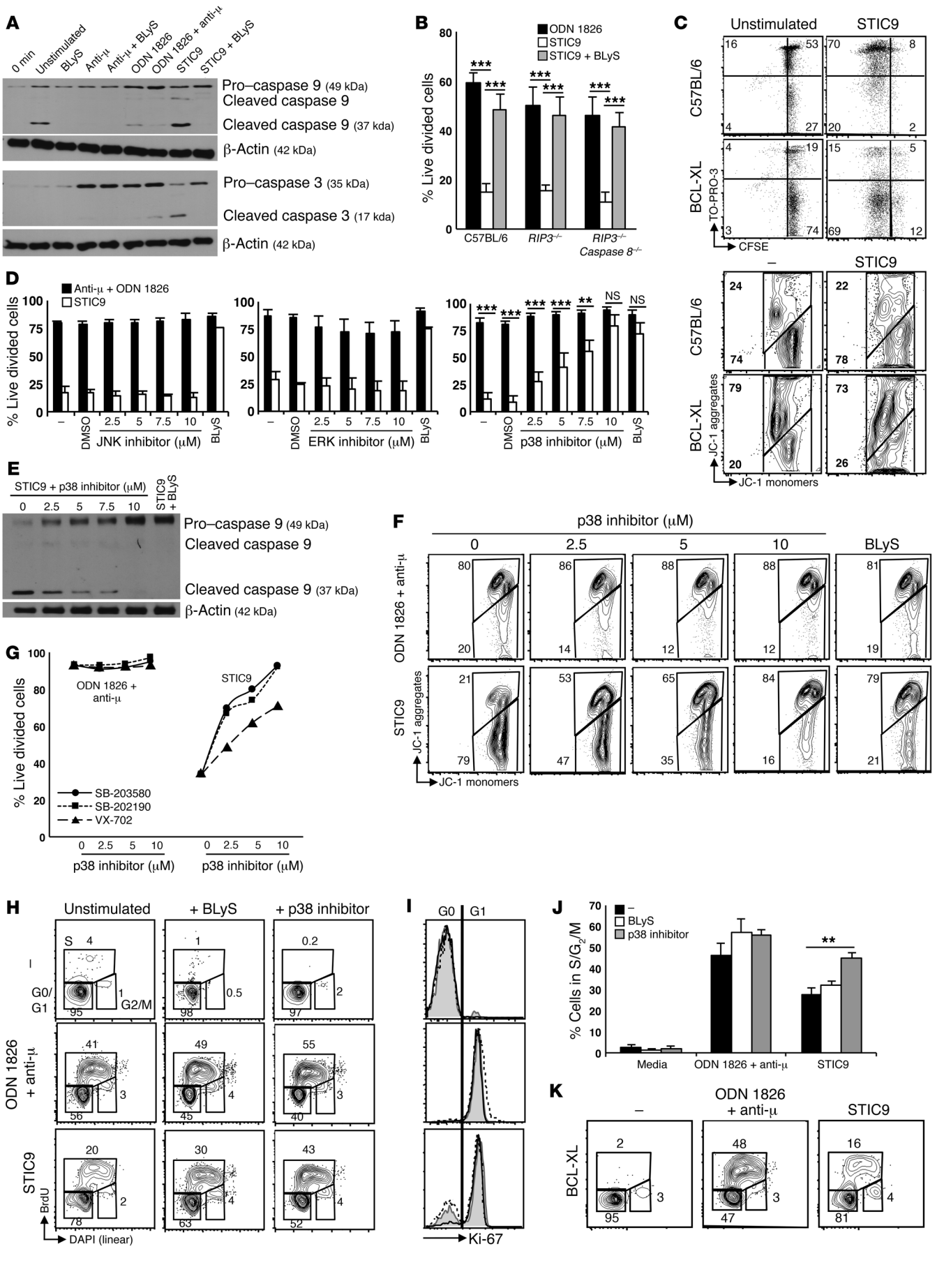

Figure 2. Cell death in response to STIC9 stimulation follows p38 MAPK–mediated cell-cycle arrest and mitochondrial apoptosis. (**A**) Immunoblot analysis of caspase 9 and caspase 3 cleavage in protein extracts from CD23$^+$ C57BL/6 splenocytes cultured for 60 hours with the indicated stimuli. Values in parentheses indicate the molecular weight. (**B**) Percentage of live divided CD23$^+$ splenocytes from C57BL/6, *RIP3*$^{-/-}$, and *RIP3*$^{-/-}$ caspase 8$^{-/-}$ mice following culture with the indicated stimuli. (**C**) Representative FACS plots of C57BL/6 and BCL-XL CD23$^+$ splenocytes cultured for 60 hours with no stimulation or with STIC9 either loaded with CFSE and stained with TO-PRO-3 or stained with the mitochondrial stability–assessing dye JC-1. (**D**) Percentage of live divided C57BL/6 CD23$^+$ splenocytes following stimulation with either anti-μ or STIC9 in the presence of various concentrations of the JNK inhibitor SP600125, the MEK1/2 inhibitor U0126, or the p38 inhibitor SB203580. Since vehicle and non-vehicle control groups showed no differences, the latter was used for controls in subsequent experiments. (**E**) Immunoblot analysis of caspase 9 cleavage as described in **A**. (**F**) Representative FACS plots assessing the mitochondrial stability of C57BL/6 CD23$^+$ cells cultured for 60 hours with the indicated stimuli. (**G**) Percentage of live divided C57BL/6 CD23$^+$ splenocytes following culture as in **D** with various p38 inhibitors. (**H** and **I**) FACS analysis measuring the cell-cycle status of C57BL/6 CD23$^+$ splenocytes cultured for 48 hours with the indicated stimuli. (**I**) G_0 and G_1 phases were distinguished through Ki-67 staining. The gray area represents STIC9 alone; the dashed line represents STIC9 plus BLyS; and the solid black line represents STIC9 plus the p38 inhibitor SB203580. (**J**) Percentage of cells in the S/G_2/M phase treated as in **H**. (**J** and **K**) FACS analysis measuring the cell-cycle status of BCL-XL–transgenic CD23$^+$ splenocytes cultured for 48 hours. Error bars indicate the mean ± SEM; $n \geq 3$ replicate analyses, and results are representative of 2 (**B** and **E**) or a minimum of 3 (**A**, **C**, **D**, and **F**–**K**) independent experiments. $^{**}P < 0.005$ and $^{***}P < 0.001$, by 2-tailed Student's *t* test. NS, not significant.

have been shown to affect B cell responses by modulating subcellular compartmentalization of TLR9 and MAPK signaling (49). Accordingly, we reasoned that STIC9 signals probably involve the MAPK pathways and asked whether inhibition of JNK, ERK, or p38 could block STIC9-induced apoptosis. Neither JNK nor ERK inhibition altered the patterns of response to ODN 1826 plus anti-μ or STIC9, despite both inducing the expected decrease in viability and proliferation with anti-μ (Figure 2D and Supplemental Figure 2E). In contrast, p38 inhibition abrogated STIC9-induced cell death, and at 10 μM, the inhibitor rescued cells to the same extent as did BLyS (Figure 2D). Further, p38 inhibition prevented the caspase 9 cleavage and mitochondrial depolarization that otherwise follow STIC9 stimulation (Figure 2, E and F). To exclude off-target effects, we used 2 additional p38 inhibitors — SB202190 and VX702 — and both rescued STIC9-driven death (Figure 2G). Thus, BCR-delivered TLR9 ligands, unlike independent BCR or TLR9 stimulation, trigger a p38-dependent mechanism that leads to intrinsic mitochondrial apoptosis.

Following activation, B cell survival requires successful cell-cycle transit, and p38 has been implicated in stress-induced cell-cycle arrest (50). To determine the effect of STIC9 on cell-cycle status, B cells were stimulated and harvested after 48 hours, a time point at which viability in all cultures is comparable (Figure 1D). As expected, 44% of B cells stimulated with ODN 1826 plus anti-μ were in the S/G_2/M phase. In contrast, the majority of cells stimulated by STIC9 were in G_1, with only 22% of the cells in S/G_2/M (Figure 2, H–J), in spite of the fact that most underwent several rounds of division (Figure 1B). Together, these findings suggest that STIC9–stimulated cells experience cell-cycle arrest at the G_1-S transition.

The addition of a p38 inhibitor reduced the proportion of cells in G_1, with a corresponding elevation of the proportion of cells in S/G_2/M (Figure 2, H–J), suggesting that STIC9 stimulation induces G_1/S cell-cycle arrest prior to mitochondrial apoptosis. However, it remained possible that cells undergoing mitochondrial apoptosis simply accumulate in the G_1 phase of the cell cycle. To address this possibility, we cultured B cells from BCL-XL mice with STIC9. Like C57BL/6 B cells, the majority of STIC9-stimulated BCL-XL transgene–positive cells were in G_0/G_1, despite their resistance to apoptosis (Figure 2K), consistent with the view that cell-cycle arrest precedes initiation of the intrinsic mitochondrial death pathway. Overall, these findings show that BCR-delivered TLR9 agonists terminate B cell activation through a p38-dependent cell-cycle arrest mechanism that subsequently drives mitochondrial cell death.

All preimmune B cell subsets undergo TLR9-dependent post-proliferative death that can be rescued by BLyS. Both transitional (TR) and marginal zone (MZ) B cells express TLR9, include autoreactive or polyreactive clonotypes, and have been implicated in humoral autoimmune disease (51–53). Therefore, to examine how BCR-delivered TLR9 ligands affect these B cell subsets, we FACS sorted FO, MZ, TR type 2/3 (TR2/3), and TR type 1 (TR1) B cells as previously defined (54, 55). In accord with prior studies, anti-μ induced death among TR and MZ B cells (Figure 3A). In contrast, all subsets divided following stimulation with ODN 1826 plus anti-μ and were alive after 60 hours in culture. Mirroring our results with magnetic cell-sorting–enriched (MACS-enriched) CD23$^+$ B cells, all subsets examined had proliferated following STIC9 stimulation and then died by 60 hours in culture (Figure 3A). Cell death in all subsets was most likely via mitochondrial intrinsic apoptosis, as cleavage of caspase 9 was observed in sorted FO, MZ, TR2/3, and TR1 B cells following STIC9 stimulation (Figure 3B). These data provide a previously unappreciated intrinsic role for TLR9 in limiting the responses of all preimmune B cell subsets to DNA-containing antigens.

BLyS allows STIC9-stimulated B cells to become antibody-secreting cells. Since B cells can be rescued from post-proliferative death by BLyS, we asked whether this or other signals enable progression to either antibody secretion or other differentiative fates. Accordingly, we first asked whether B cells stimulated with STIC9 and kept alive by BLyS could become antibody-secreting cells. As expected, CD23$^+$ B cells cultured with BLyS alone secreted minimal antibody, however, both TR and FO subsets secreted 10-fold more antibody following stimulation with either ODN 1826 plus anti-μ or STIC9 plus BLyS (Table 1 and Figure 4A, upper panel). Supernatants from MZ B cells revealed a similar pattern of Ig secretion, albeit at a greater magnitude, consistent with their vigorous response to TLR stimuli and propensity to undergo rapid plasma cell differentiation (56). Moreover, enzyme-linked immunosorbent spot (ELISPOT) analyses confirmed that ODN 1826 plus anti-μ or STIC9 plus BLyS induced antibody-secreting cell (ASC) formation (Figure 4A, lower panel). Importantly, lambda$^+$ B cells from 3H9 BCR–transgenic mice, which are dsDNA specific and normally eliminated at the TR stage (17, 57–60), were able to differentiate into ASCs following stimulation with STIC9 plus BLyS (Supplemental Figure 3C). These data reveal that TLR9 ligands delivered via the BCR yield a similar, self-limiting response by all major peripheral B cell subsets and that concomitant survival signals permit continued differentiation into ASCs.

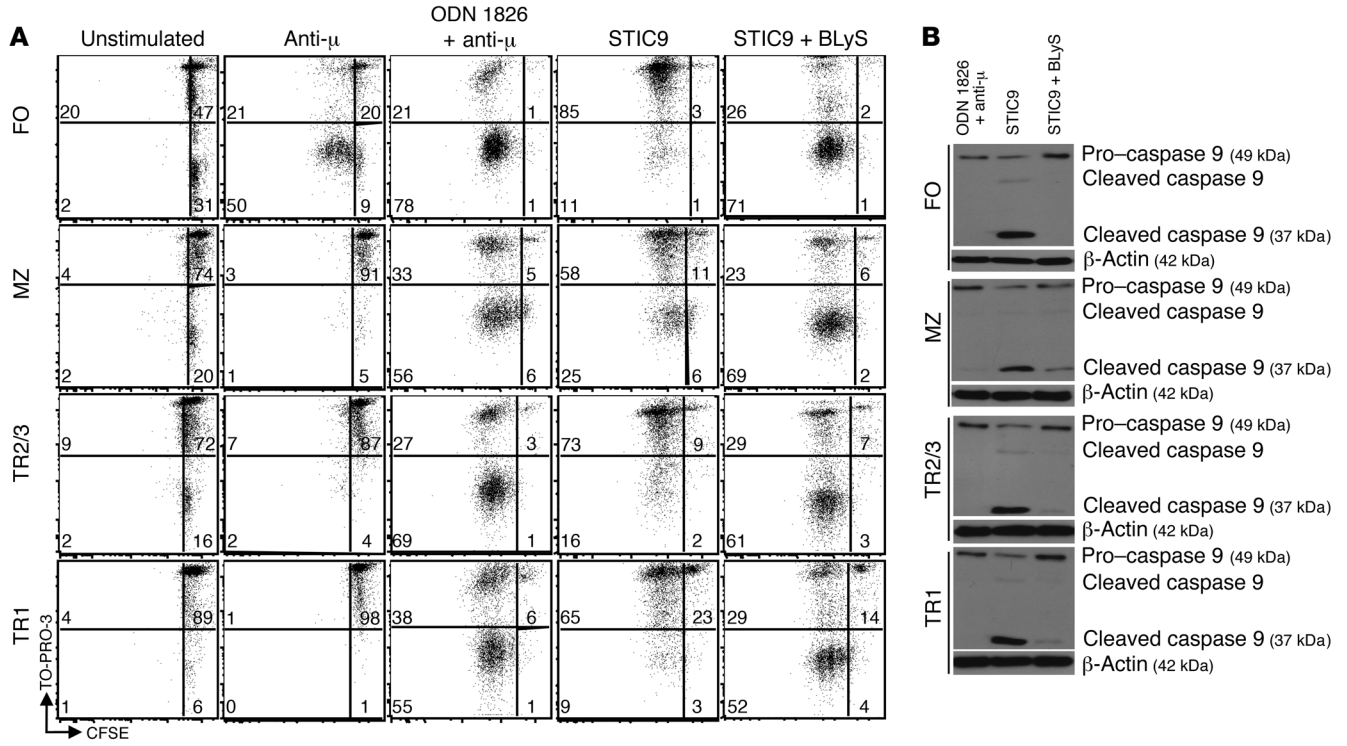

Figure 3. FO, MZ, and TR B cells behave similarly following STIC9 stimulation. (**A**) FACS analysis of proliferation and survival in sorted B220$^+$AA4.1$^-$CD23$^+$CD21/35$^-$ FO, B220$^+$AA4.1$^-$CD23$^-$CD21/35$^+$ MZ, B220$^+$AA4.1$^+$CD23$^+$ TR2/3, and B220$^+$AA4.1$^+$CD23$^-$ TR1 splenic B cells cultured for 60 hours with no stimulation, with F(ab′)$_2$ fragments of anti-IgM, with ODN 1826 plus F(ab′)$_2$ fragments of anti-IgM, STIC9, or with STIC9 plus BLyS. Dead cells were stained by TO-PRO-3, while CFSE dilution indicates proliferation. (**B**) Immunoblot analysis of caspase 9 cleavage in protein extracts isolated from FO, MZ, TR2/3, and TR1 B cells cultured for 60 hours with ODN 1826 plus F(ab′)$_2$ fragments of anti-IgM, STIC9, or STIC9 plus BLyS. Protein (10 μg) was loaded into each well, and β-actin was used as a loading control. Values in parentheses indicate the molecular weight. All data are representative of 3 (**A**) or 2 (**B**) independent experiments.

CD40 costimulation and FO helper T cell cytokines rescue TLR9-dependent post-proliferative death and foster a T-bet$^+$ fate. Although BLyS allows STIC9-stimulated B cells to survive and differentiate into ASCs, we reasoned that alternative second signals — such as CD40 costimulation and instructive cytokines characteristic of T cell-dependent immune responses — might foster alternative differentiative fates. Moreover, because T-bet expression and IgG$_{2a/c}$ isotype switching are regulated by IL-21, IFN-γ, and IL-4 in the context of TLR9 signals (35), we speculated that these features might extend to STIC9-stimulated cells. Accordingly, we assessed the effects of CD40 costimulation in the context of IL-21, IFN-γ, and IL-4 on the survival and differentiative outcomes of STIC9-stimulated B cells.

CD40 signaling alone mirrored the findings with BLyS, rescuing the cells and enabling antibody secretion (Figure 4, A and B). The added presence of IFN-γ, IL-21, or IL-4 did not affect CD40-mediated rescue (Figure 4B, upper panel). We reasoned that during B cell responses in vivo, CD40 signals would be delayed with respect to BCR-mediated activation, reflecting the need for B cell antigen processing and presentation to receive cognate T cell help. We therefore assessed rescue by CD40 signals delivered 24 or 48 hours after STIC9 stimulation. The results indicated that CD40 signals received within 24 hours of STIC9 stimulation yield equivalent rescue when these signals are received simultaneously and that even 48 hours after STIC9 stimulation, CD40 ligation affords partial rescue (Figure 4B, lower panel).

In accord with previous reports, both T-bet expression and IgG$_{2c}$ class switching increased markedly when either IFN-γ or IL-21 (Figure 4, C–G) was added in conjunction with CD40 ligation; whereas, IL-4 fostered neither T-bet expression nor IgG$_{2c}$ switching but instead yielded IgG$_1$ production. As shown previously in the context of TLR9 signaling (35), the induction of T-bet

Table 1. Antibody production by cells cultured with STIC9 and BLyS

Splenic B cell subset	Culture conditions		
	BLyS	ODN 1826 + anti-μ	STIC9 + BLyS
FO	4 ± 1	113 ± 27^B	66 ± 25^A
MZ	20 ± 4	2,905 ± 2,392	4,230 ± 336^B
TR2/3	10 ± 5	199 ± 45^B	134 ± 45^B
TR1	11 ± 3	159.3 ± 40^B	167 ± 44^B

Mean ± SD of total Ig (ng/ml) in supernatants from sorted subsets cultured for 60 hours. n = 3 independent experiments. A 2-tailed Student's t test was used for the statistical analysis. ^{A}Denotes significant differences at $P < 0.05$ for stimulation with BLyS alone. ^{B}Denotes significant differences at $P < 0.01$ for stimulation with BLyS alone.

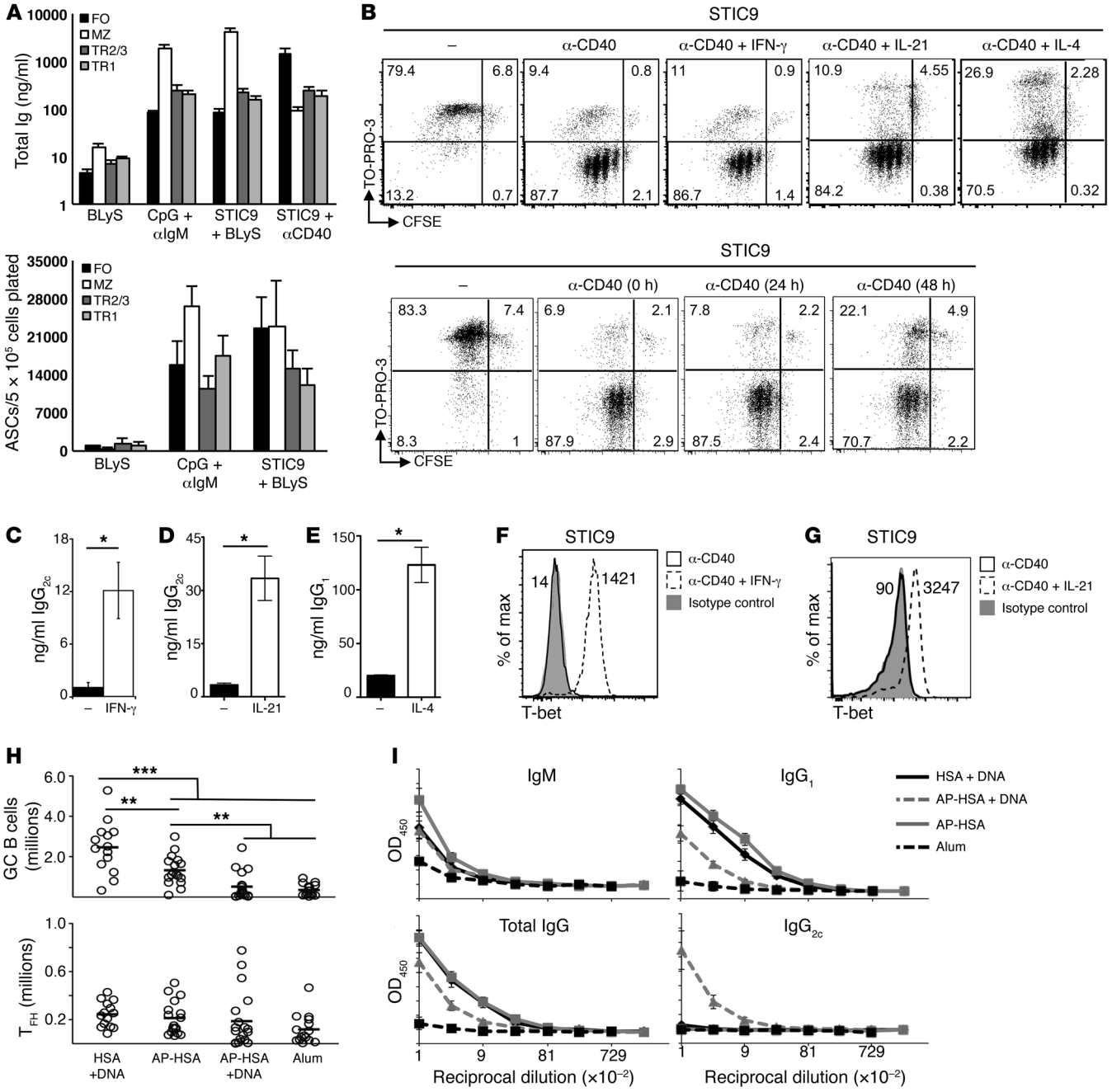

Figure 4. CD40 and Tfh cytokines promote survival, T-bet expression, and IgG_{2c} class-switching in STIC9-stimulated cells, and DNA conjugation modulates T cell-dependent B cell responses in vivo. (**A**) Sort-purified FO, MZ, TR2/3, and TR1 B cells cultured for 60 hours with the indicated stimuli. Total Ig was measured in the supernatants by ELISA, and total ASCs were measured by ELISPOT. Each stimulation group (CpG plus anti-IgM, STIC9 plus BLyS, and STIC9 plus anti-CD40) induced significantly more ($P < 0.05$) total Ig or ASCs compared with BLyS stimulation alone when compared with the respective B cell subsets. (**B**) FACS analysis of the proliferation and survival of FO B cells cultured for 60 hours with the indicated cytokines and anti-CD40 added simultaneously with STIC9 stimulation (upper panels), or with anti-CD40 added at different time points after STIC9 stimulation (lower panels). (**C**–**E**) FO B cells were cultured with STIC9 plus anti-CD40, with or without (**C**) IFN-γ, (**D**) IL-21, or (**E**) IL-4 for 60 hours, following which (**C** and **D**) IgG_{2c} and (**E**) IgG1 were measured by ELISA. (**F** and **G**) FO B cells were cultured with STIC9 plus anti-CD40, with or without (**F**) IFN-γ or (**G**) IL-21 for 60 hours, and cells were probed for T-bet by intracellular flow staining. Plots show T-bet expression in live cells. Numbers inside the plots indicate the Δ mean fluorescence intensity (MFI) (experimental minus isotype control). (**H**) Total number of splenic GC B cells [DUMP(CD4, CD8, GR-1, F4/80)$^-$IgD$^{lo/-}$CD19$^+$CD138$^-$CD38$^-$GL7$^+$FAS$^+$] and Tfh cells (CD19$^-$CD4$^+$CD62L$^{lo/-}$CXCR5^{hi}PD-1^{hi}) present in the indicated immunized C57BL/6 mice on day 14 after immunization. Each symbol represents an individual mouse. ANOVA with Bonferroni's correction was used for multiple comparisons. (**I**) HSA-specific serum titer in the indicated immunized mice on day 14 after immunization. All data are representative of 2 (**A**) or 3 (**B**–**I**) independent experiments. (**C**–**E**) Error bars indicate the mean ± SEM. *P <0.05, **P < 0.005, and ***P < 0.001, by 2-tailed Student's t test.

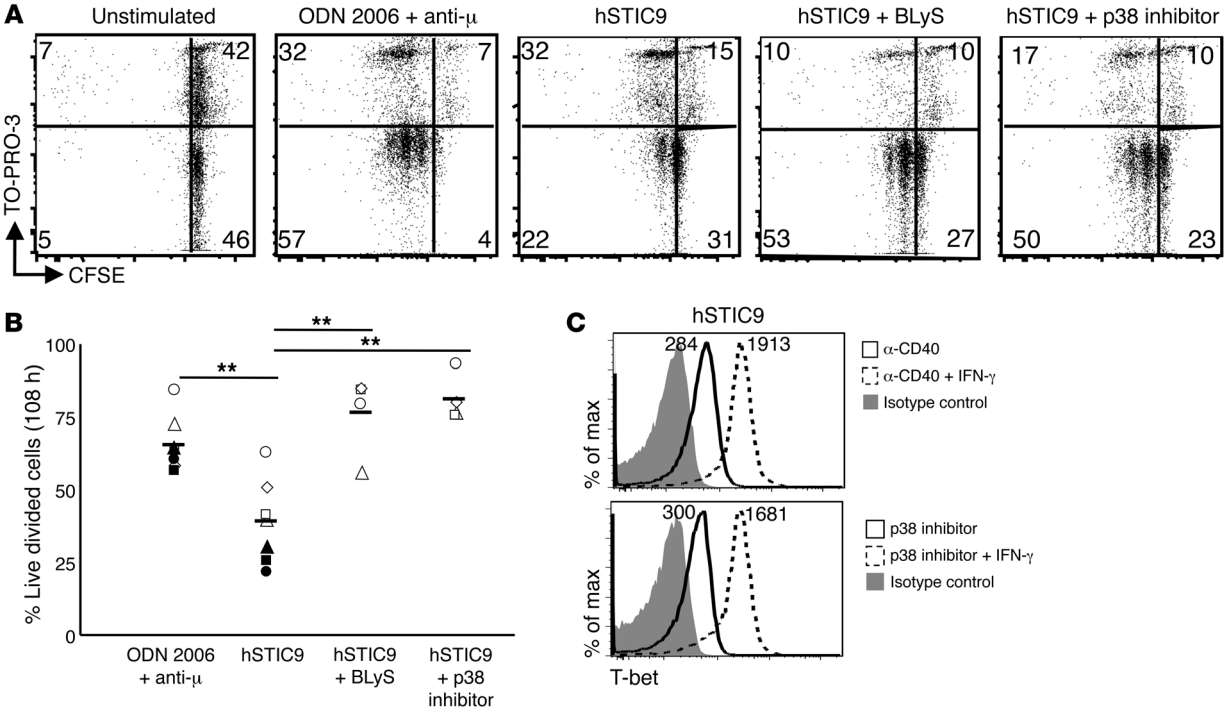

Figure 5. Naive human B cells undergo post-proliferation apoptosis following stimulation with BCR-internalized TLR9 ligands. (**A**) Representative FACS plots showing proliferation and survival in human $CD27^-CD19^+$ PBMCs cultured for 108 hours with no stimulation, ODN 2006 plus $F(ab')_2$ fragments of anti-IgM, hSTIC9, hSTIC9 plus BLyS, or hSTIC9 plus SB203580. Dead cells were stained by TO-PRO-3, while CFSE dilution indicates proliferation. (**B**) Percentage of live divided cells from multiple donors treated as in **A**. Each symbol represents a single donor. Black symbols (n = 3) indicate cells that were cultured with ODN 2006 plus $F(ab')_2$ fragments of anti-IgM and hSTIC9, while white symbols (n = 4) indicate cells that were additionally cultured with hSTIC9 plus BLyS or hSTIC9 plus the p38 inhibitor SB203580. (**C**) Human $CD27^-CD19^+$ PBMCs were cultured with STIC9 plus p38 inhibitor (10 μM) or STIC9 plus anti-CD40, with or without IFN-γ, for 108 hours. At the end of the culture, cells were stained for T-bet. Plots show T-bet expression in live cells. Numbers inside the plot indicate Δ MFI (experimental minus isotype control). n = 3 for all data, and results are representative of at least 3 independent experiments. $^{**}P < 0.005$, by 2-tailed Student's t test.

expression by IFN-γ and IL-21 occurs within the first 24 hours of activation and is independent of the extent to which B cells have divided after STIC9 plus anti-CD40 stimulation (Supplemental Figure 3, A and B).

Antigen-complexed DNA yields blunted humoral responses with T-bet⁺ B cell–associated characteristics. Considered together, these in vitro analyses predicted that TLR9 agonists delivered by the BCR should limit B cell responses. We reasoned that in the absence of additional signals, incipient responses to DNA-containing antigens should prematurely terminate, whereas the presence of additional signals such as cognate CD4 help and cytokines should modulate the response and determine its quality. We used immunization with amyloid proteins to test this hypothesis in vivo. These misfolded proteins form fibrous structures termed amyloid aggregates, sometimes including cofactors such as DNA (61), and we have previously reported a method to produce amyloid proteins with or without DNA (61, 62). Using this approach, we immunized mice with amyloid precursor HSA (AP-HSA), AP-HSA linked to DNA, or native HSA mixed with, but not cross-linked to, DNA. Alum was used as an adjuvant in all conditions, and we also included an adjuvant-only control. On day 14 after immunization, mice receiving HSA plus DNA or AP-HSA had mounted an immune response with germinal center (GC) B cells, FO helper T cells (Tfh) (Figure 4H), and IgG_1 antibody (Figure 4I). In contrast, immunization with AP-HSA plus DNA yielded reduced GC B cell numbers that were equivalent to those detected with adjuvant only, as well as reduced titers of class-switched HSA-specific antibodies that were skewed toward IgG_{2c} (Figure 4, H and I). Interestingly, Tfh numbers were normal with this immunization (Figure 4H). Immunization with AP-HSA plus DNA ICs yielded a reduction in GC B cell numbers, but not complete ablation of the response. This finding is in agreement with our in vitro observations (Figure 4, A and B) suggesting that CD40 ligation affords rescue even several days after B cell activation by BCR ligands that contain a TLR9 agonist. Together, these findings are consistent with the overall relationships established by our in vitro analyses, since complexed DNA modulates the humoral response and, in the presence of cognate help, engenders the IgG_{2c} isotype–switching characteristic of T-bet induction.

BCR-delivered TLR9 ligands limit human $CD27^-$ B cell responses. Finally, we questioned whether human B cells are similarly regulated by DNA-containing antigens. Human TLR9 signals optimally to a different CpG motif than does murine TLR9, but this motif appears in the clone 11 sequence that we used in STIC9. Therefore, we designed a human stimulatory TLR9 complex (hSTIC9) by linking biotinylated clone 11 to biotinylated Fab anti-human IgM with SA. Naive ($CD27^-CD19^+$) human B cells were isolated and cultured for 108 hours, when proliferative responses most closely resembled those seen after 60 hours with murine $CD23^+$ B cells (Figure

5A). As expected, the majority of human B cells cultured with ODN 2006 plus F(ab′)$_2$ anti-human IgM were alive and had proliferated (Figure 5, A and B). Mirroring the response of murine B cells, human B cells stimulated with hSTIC9 underwent a proliferative burst followed by apoptosis, and either BLyS addition or p38 inhibition rescued this death (Figure 5, A and B). Moreover, when human B cells were rescued from death, they expressed T-bet, which was further enhanced in the presence of IFN-γ (Figure 5C). These findings strongly suggest that human and murine preimmune B cells undergo similar responses to BCR-delivered TLR9 ligands and that these probably reflect similar molecular mechanisms.

Discussion

This study reveals a relationship among BCR, TLR9, and cytokine signals that regulate B cell responses to DNA-containing antigens. BCR ligands that deliver a TLR9 agonist yield a brief proliferation that is terminated by cell-cycle arrest and intrinsic apoptotic death. This self-limiting response is characteristic of all major preimmune B cell subsets in mice and humans and requires MAPK p38 activation. BLyS prolongs this otherwise short-lived response, enabling the activated B cells to survive and differentiate into ASCs, whereas CD40 costimulation and Tfh cytokines yield both antibody secretion and differentiation into the autoimmune-associated T-bet$^+$ B cell phenotype. Together, these observations disclose a mechanism that prevents or limits responses to DNA-associated BCR ligands and may help explain how TLR9 deficiency promotes humoral autoimmunity.

The proapoptotic role of TLR9 shown here is seemingly at odds with an extensive literature showing that TLR9 agonists engender B cell division without cell death and are effective vaccine adjuvants (63). However, TLR9 signaling in these contexts likely differs from the BCR-mediated internalization of natural ICs or STIC9, as such small molecules do not involve BCR engagement in their uptake (64, 65). In addition, TLRs can signal from a range of endolysosomal compartments with varying functional outcomes (66, 67). Studies of simultaneous engagement of BCR and TLR9, similar to STIC9, showed that BCR and TLR9 colocalize in autophagosomes and initiate the hyperphosphorylation of p38 MAPK after such activation. Results of these studies also demonstrated the unique signaling pathways by which B cells regulate responses to DNA-containing antigens, namely, by governing the subcellular location of TLR9 and MAPK signaling (49, 68). Whether free CpG ODNs reach the same compartment as BCR-delivered TLR9 ligands is unclear, but CpG ODN and ICs elicit different cytokines from AM14 B cells (48), consistent with fundamentally different signaling outcomes. Further, while the affinity of TLR9 for DNA components of different ligands is a potentially confounding factor, ODN 1826 engenders post-proliferative death when conjugated to F(ab′)$_2$ anti-μ, favoring the interpretation that BCR-mediated delivery is the key distinction. Similarly, BCR engagement and signal strength might also impact outcome. However, multiple measures of BCR signal strength indicate that BCR signals induced by each reagent used herein are comparable and further support the notion that BCR-associated delivery of the TLR9 agonist underlies this unique response.

The STIC9 reagent affords the separation of BCR-mediated proliferative signals from TLR9-dependent cell death, thus enabling interrogation of the downstream pathways. While one might argue that a dominant, TLR9-mediated death pathway is involved, this seems unlikely, because simultaneous but independent ligation of TLR9 and the BCR does not result in cell death. Instead, we favor the notion that crosstalk between these systems is responsible, whereby TLR9 ligation impedes or redirects survival signals that otherwise accompany BCR signaling. The exact points of intersection remain unclear, but engagement of both the BCR and TLR9 initiates the NF-κB and MAPK pathways, so crosstalk between these, including the documented hyperactivation of p38 (49), likely plays a role in the post-proliferative death mechanism reported herein. Indeed, our findings reveal a central role for p38 in STIC9-induced cell-cycle arrest and mitochondrial apoptosis, functions that have previously been associated with the p38 pathway (69–71). Cell-cycle arrest and mitochondrial apoptosis may reflect parallel but independent consequences of p38 signaling following stimulation with BCR-delivered TLR9 ligands. Alternatively, as cell-cycle arrest occurs even when apoptosis is blocked, it may be a proximal event that leads directly to mitochondrial destabilization. Regardless, both reflect potential limiting mechanisms that prevent continued expansion or prolonged survival of autoreactive B cell clones.

The TLR9-mediated post-proliferative death response that we observed is likely relevant to the etiology of humoral autoimmunity. For example, it may help explain why TLR9-deficient autoimmune strains develop more severe disease than do their TLR9-sufficient counterparts (15, 16, 18–20). Consistent with this notion, autoimmune disease is similarly exacerbated when TLR9 deficiency is limited to B cells (72). Nevertheless, in addition to its negative regulatory role, TLR9 is also required for B cell activation, ASC differentiation, and the production of isotype-switched, DNA-reactive autoantibodies in autoimmune-prone mice (15, 32). Further, this unique response — an initial proliferative burst followed by rapid elimination — is common to all major preimmune subsets in mice and humans. This suggests that TR and MZ B cells, which contain polyreactive and autoreactive clones, could be recruited to clear TLR9-containing BCR ligands such as apoptotic debris, but are quickly eliminated to avoid sustained activity against self-components. Alternatively, this mechanism might be important for purging self-reactive B cells at the immature and TR stages. In fact, in 3H9 mice, either exogenous BLyS or TLR9 deficiency extends the lifespan of dsDNA-specific B cells normally lost at the TR stage (17, 59), and mutations impacting TLR9 function are associated with a more polyreactive B cell repertoire (73). These possibilities are not mutually exclusive and could both serve as checkpoints in the prevention of autoimmune disease.

Impeding the TLR9-mediated post-proliferative death response through either intrinsic failure in the relevant pathways or misdirected survival and differentiation signals could increase the propensity for autoimmune pathogenesis, and it is tempting to speculate that these differences might lead to distinct risk and disease features. For example, circumventing this mechanism through excess BLyS might afford the formation of short-lived autoreactive plasmablasts. Indeed, BLyS depletion therapy has had mixed success in ameliorating systemic lupus erythematosus (SLE) flares, perhaps reflecting restoration of this pathway in a subset of patients (24). In contrast to BLyS, T cell–mediated rescue of BCR-TLR9 coengagement might

foster GC differentiation, allowing somatic hypermutation, affinity maturation, and the generation of long-lived plasma or memory B cells. This is supported by our observations that addition of anti-CD40 with the IL-21 and IFN-γ cytokines engenders survival and induces T-bet expression and class-switching to $IgG_{2a/c}$. Since T-bet$^+$ B cells have been reported in the context of aging, autoimmunity, and infections (74), these cells may arise in response to TLR9 ligands delivered via the BCR, and while such signals would ordinarily trigger apoptosis, cognate T cell help and additional cytokines could result in the breakthrough of autoantibody production. Additionally, in vivo and in vitro data suggest that RNA-sensing receptors, such as TLR7, do not promote post-proliferative cell death, but instead foster plasma cell differentiation (75). Thus, activation via these pathways may require concomitant TLR9 signals to control the overall response (30, 33, 76). Indeed, in mouse models in which TLR7 plays a critical role, TLR9 haploinsufficiency exacerbates disease (15, 16, 18–20). Finally, some B cell subsets may resist this mechanism. Our preliminary observations indicate that CD27$^+$ human B cells may resist hSTIC9-driven post-proliferative death, suggesting that some memory B cell subsets are refractory. Thus, TLR9 may play a unique role in limiting the duration of potentially autoreactive responses, and alternative routes for bypassing this regulatory system may underlie some of the variability in the clinical features and therapeutic outcomes observed in humoral autoimmunity.

Methods

Mice. C57BL/6 and *Nur77-GFP* reporter mice (77) were purchased from the The Jackson Laboratory. AM14 mice were maintained at the University of Massachusetts. *Tlr9*$^{-/-}$ mice were provided by P. Scott (University of Pennsylvania). *Taci*$^{-/-}$ (78), 3H9-transgenic, and B cell–specific BCL-XL–transgenic (79) mice were maintained at the University of Pennsylvania. BR3-deficient mice were maintained at the University of Southern California (Los Angeles, California, USA). Caspase 8$^{-/-}$*RIP3*$^{-/-}$ and *RIP3*$^{-/-}$ mice were provided by William Kaiser and Edward Mocarski (Emory University, Atlanta, Georgia, USA).

B cell cultures. B cells were collected from 8- to 16-week-old male and female mice. Splenic B cells were isolated by positive selection and cultured as described previously (38, 39, 44, 76, 80). Briefly, B cells were stimulated with 10 micrograms/ml $F(ab)'_2$ fragments of goat anti-IgM (Jackson ImmunoResearch Laboratories); 1 μg/ml anti-CD40 (clone HM40-3; BD); and 1 μM CpG DNA (ODN 1826; InvivoGen). STIC9 ICs were formed by combining a biotinylated CG-rich dsDNA fragment (39) with SA and Fab anti-mouse IgM at a final concentration of 0.5 μg/ml dsDNA, 0.13 μg/ml SA, and 0.5 μg/ml Fab anti-mouse IgM. Murine IL-21, IL-4, and IFN-γ (Shenandoah Biotechnology Inc.) were used at 25, 10, and 10 ng/ml, respectively. Human peripheral blood mononuclear cells (PBMCs) were isolated through negative selection with magnetic anti-human CD27 beads, followed by positive selection with anti-human CD19 beads (Miltenyi Biotec) and cultured in round-bottomed plates for 108 hours. Cells were loaded with CFSE (Invitrogen, Thermo Fisher Scientific) as described previously (44). Human PBMCs were collected from both healthy men and women, aged 28–52 years. Inhibitor studies used 2.5–10 μM SB203580 (InvivoGen); SB202190 (Cell Signaling Technology); VX-702 (Cayman Chemical); U0126 (Cell Signaling Technology); or SP600125 (InvivoGen). Stimulations had 500 ng/ml recombinant human BLyS (rhBLyS) (Human Genome Sciences Inc. or R&D Systems); 10 μg/ml $F(ab')_2$ anti–human IgM (Jackson ImmunoResearch Laboratories); 1 μM CpG DNA (ODN 2006; InvivoGen); or hSTIC9, formed by combining 1 μg/ml biotinylated clone 11 DNA; 0.5 μg/ml SA (New England Biolabs); and 0.25 μg/ml Fab anti-human IgM, $FC_{5\mu}$ fragment specific (Jackson ImmunoResearch Laboratories) for 1 hour at 4°C.

Flow cytometry. For all analyses, live/dead discrimination was assessed using either a LIVE/DEAD Fixable Aqua Stain Kit, DAPI, or TO-PRO-3 (Invitrogen, Thermo Fisher Scientific). Spleens were disrupted to single-cell suspensions and red blood cells lysed using ammonium-chloride-potassium (ACK) buffer (Lonza). Fluorochrome-conjugated or biotinylated antibodies against mouse CD19 (clone 6D5), B220 (clone RA3-6B2), CD21/CD35 (clone CR2/CR1), AA4.1/CD93 (clone AA4.1), IgD (clone 11–26c.2a), CD138 (clone 281-2), CXCR5 (clone L138D7), PD-1 (clone RMP1-30), TCRβ (clone H57-597), and T-bet (clone 4B10) were purchased from BioLegend; CD23 (clone B3B4), IgM (clone R6-60.2), CD95 (clone Jo2), and CD62L (clone MEL-14) from BD Biosciences; and CD4 (clone RM4-5), CD8 (clone 53-6.7), F4/80 (clone BM8), GR-1 (clone RB6-8C5), and CD38 (clone 90) from eBioscience. Cells were stained with antibodies in PBS/1% BSA containing mouse IgG Fc fragments (Jackson ImmunoResearch Laboratories). Mouse IgG1, κ antibody (clone MOPC-21; BioLegend) was used as an isotype control for T-bet staining, as described previously (35). BR3 and TACI were detected with anti-mouse BR3 (clone eBio7H22-E16; eBioscience) or anti-mouse TACI (clone 8F10; R&D Systems), with rat IgG1, κ antibody (clone eBRG1; eBioscience) and rat IgG2a, κ antibody (clone RTK2758; R&D Systems), respectively, as isotype controls. All stains were incubated for 30 minutes at 4°C, except for CXCR5, which was added first and incubated at room temperature for 1 hour. Staining with biotinylated antibodies was followed by staining with Brilliant Violet 650–conjugated SA (BioLegend). Data were collected on a BD LSR II Flow Cytometer and analyzed with FlowJo software (Tree Star).

Mitochondrial membrane potential. Mitochondrial membrane potential was analyzed by staining with JC-1 (BD Biosciences) according to the manufacturer's protocol.

Cell-cycle analysis. Cells were pulsed with 50 μg/ml BrdU for the last 90 minutes of cell culture; fixed and permeabilized using BD Cytofix Solutions A and B (BD Bioscience); incubated with 225 μg/ml DNase solution in 150 mM NaCl and 400 mM $MgCl_2$ for 35 minutes at room temperature; and stained with FITC anti-BrdU antibody (B44; BD Bioscience) and DAPI. G_0/G_1 was differentiated with anti–Ki-67 (16A8; BioLegend).

Immunoblot analysis. Lysates were prepared and separated by SDS-PAGE as described previously (81, 82). Proteins were quantified by a Bio-Rad assay (Bio-Rad). Protein (10 μg) was loaded into each well, and β-actin was used as a loading control. Immunoblots were performed using rabbit anti-mouse caspase 9, rabbit anti-mouse caspase 3, or rabbit anti-mouse phosphorylated SYK (p-SYK) (all from Cell Signaling Technology). Peroxidase-conjugated donkey anti-rabbit IgG (H+L) (Jackson ImmunoResearch) was used as a secondary detection antibody. Peroxidase-conjugated mAb against mouse β-actin (AC-15; Sigma-Aldrich) was used as a loading control. Quantity One 1-D Analysis Software (Bio-Rad) was used for gel densitometry.

ELISA and ELISPOT analyses. Plates were coated with 10 μg/ml anti-Ig (H+L) (SouthernBiotech) as previously described (83). For ELISA, culture supernates were plated and incubated with secondary HRP-conjugated goat anti-mouse Igκ plus anti-mouse Igλ antibodies

(SouthernBiotech). Plates were analyzed as previously described (83). For ELISPOTs, cells that had been cultured for 48 hours were replated and cultured for 8 hours at 37°C, then developed with biotin-conjugated anti-mouse Igκ plus anti-mouse Igλ (SouthernBiotech) as previously described (83). Plates (Corning) were coated overnight with 1 μg/ml native HSA and blocked for 2 hours in PBS/2% BSA. Sera were added to the first row of plates at a 1:100 dilution, with serial 3-fold dilutions down the rows. Anti-HSA antibodies were detected with goat anti-mouse IgG, IgG_1, IgG_{2c}, and IgM conjugated with HRP (SouthernBiotech). TMB Substrate Reagent (BD) was used to detect HRP activity, and 2 M sulfuric acid (J.T. Baker) was used to stop the reaction. Plates were read at OD_{450} on an EMax Microplate Reader (Molecular Devices).

Preparation of amyloid and immunization. AP-HSA was prepared as previously described (62). Briefly, HSA (Sigma-Aldrich) was incubated for 2 hours in EDC (1-ethyl-3-[3-dimethyl-aminopropyl] carbodiimide hydrochloride) (Sigma-Aldrich) at a ratio of 1:5 (w/w). The mixture was neutralized by adding 10% (v/v) of 1 M Tris-HCl (Invitrogen, Thermo Fisher Scientific) at pH 10.5 and then dialyzed overnight into sterile PBS. To produce AP-HSA plus DNA, AP-HSA was incubated for more than 2 hours with *E. coli* K12 genomic DNA (InvivoGen) at a 7:3 (w/w) ratio of protein to DNA. As a control for an immunogen containing unlinked DNA and protein, native HSA was mixed with DNA at a 7:3 (w/w) ratio. Each preparation was precipitated in aluminum potassium sulfate (Thermo Fisher Scientific) at 0.25 mg/ml 10% alum solution. The pH was adjusted to 6.5, and precipitates were resuspended in sterile PBS. Mice were immunized i.p. with 70 μg protein, and spleens and sera were collected upon sacrifice 14 days later.

Statistics. All data are represented as the mean ± SEM. Statistical analysis was performed using a 2-tailed, equal-variance Student's *t* test. ANOVA analysis with Bonferroni's correction was used for multigroup comparisons in Figure 4H. A *P* value of less than 0.05 was considered statistically significant.

Study approval. Mice were handled according to a protocol approved by the IACUC of the University of Pennsylvania and the Animal Care and Use Review Office of the US Army Medical Research and Materiel Command (AMRMC). Human samples were obtained from the University of Pennsylvania Human Immunology Core, which maintains an IRB-approved protocol for secondary use of deidentified human donor specimens. Use of these cells in this study did not constitute human subjects research as defined by the NIH, and exempt determinations were made by the IRB of the University of Pennsylvania and the US AMRMC Office of Research Protections, Human Research Protection Office.

Author contributions

VJS, MAO, KM, MN, LEH, LZ, NG, KN, AMS, SDE, and AM performed experiments; MPC, AMR, WS, WC, and TK helped design experiments and provided reagents; and MAO, VJS, MPC, and AMR wrote the manuscript.

Acknowledgments

We thank Eline Luning Prak and Andrew Wells (University of Pennsylvania, Philadelphia, PA) for their valuable technical advice. We also thank Chandra Mohan and Yong Du (University of Houston, Houston, TX) for providing spleens from Sle1, Sle2, and Sle3 mice. This work was supported by the Office of the Assistant Secretary of Defense for Health Affairs, through the Peer Reviewed Medical Research Program (award nos. W81WWX-WH-10-1-0185 and W81XWH-14-1-0305 to MPC). Opinions, interpretations, conclusions and recommendations are those of the authors and are not necessarily endorsed by the Department of Defense. This work was also supported by the National Institute of Arthritis and Musculoskeletal and Skin Diseases (NIAMS), NIH grant PO1 AR-050256 (to AMR); and NIH grant R01 AR-050193 (to WS). MAO was supported in part by NIH Training Grant T32 AI-055428. NG and KM were supported in part by NIH Training Grant T32 AI-07309. KM was supported in part by NIAMS, NIH grant F31 AR-063597.

Address correspondence to: Michael P. Cancro, Department of Pathology and Laboratory Medicine, University of Pennsylvania, Perelman School of Medicine, Philadelphia, Pennsylvania 19104-6082, USA. Phone: 215.898.8067; E-mail: cancro@mail.med.upenn.edu.

1. Erikson J, Radic MZ, Camper SA, Hardy RR, Carmack C, Weigert M. Expression of anti-DNA immunoglobulin transgenes in non-autoimmune mice. *Nature*. 1991;349(6307):331–334.
2. Nemazee DA, Bürki K. Clonal deletion of B lymphocytes in a transgenic mouse bearing anti-MHC class I antibody genes. *Nature*. 1989;337(6207):562–566.
3. Meffre E, Wardemann H. B-cell tolerance checkpoints in health and autoimmunity. *Curr Opin Immunol*. 2008;20(6):632–638.
4. Tiller T, Tsuiji M, Yurasov S, Velinzon K, Nussenzweig MC, Wardemann H. Autoreactivity in human IgG^+ memory B cells. *Immunity*. 2007;26(2):205–213.
5. Wardemann H, Yurasov S, Schaefer A, Young JW, Meffre E, Nussenzweig MC. Predominant autoantibody production by early human B cell precursors. *Science*. 2003;301(5638):1374–1377.
6. Hiepe F, Dörner T, Hauser AE, Hoyer BF, Mei H, Radbruch A. Long-lived autoreactive plasma cells drive persistent autoimmune inflammation. *Nat Rev Rheumatol*. 2011;7(3):170–178.
7. Zaheen A, Martin A. Activation-induced cytidine deaminase and aberrant germinal center selection in the development of humoral autoimmunities. *Am J Pathol*. 2011;178(2):462–471.
8. Diamond B, Katz JB, Paul E, Aranow C, Lustgarten D, Scharff MD. The role of somatic mutation in the pathogenic anti-DNA response. *Annu Rev Immunol*. 1992;10:731–757.
9. Jiang C, et al. Abrogation of lupus nephritis in activation-induced deaminase-deficient MRL/lpr mice. *J Immunol*. 2007;178(11):7422–7431.
10. Shlomchik M, et al. Anti-DNA antibodies from autoimmune mice arise by clonal expansion and somatic mutation. *J Exp Med*. 1990;171(1):265–292.
11. Kotzin BL. Systemic lupus erythematosus. *Cell*. 1996;85(3):303–306.
12. Green NM, Marshak-Rothstein A. Toll-like receptor driven B cell activation in the induction of systemic autoimmunity. *Semin Immunol*. 2011;23(2):106–112.
13. Groom JR, et al. BAFF and MyD88 signals promote a lupuslike disease independent of T cells. *J Exp Med*. 2007;204(8):1959–1971.
14. Mackay F, et al. Mice transgenic for BAFF develop lymphocytic disorders along with autoimmune manifestations. *J Exp Med*. 1999;190(11):1697–1710.
15. Christensen SR, Kashgarian M, Alexopoulou L, Flavell RA, Akira S, Shlomchik MJ. Toll-like receptor 9 controls anti-DNA autoantibody production in murine lupus. *J Exp Med*. 2005;202(2):321–331.
16. Christensen SR, Shupe J, Nickerson K, Kashgarian M, Flavell RA, Shlomchik MJ. Toll-like receptor 7 and TLR9 dictate autoantibody specificity and have opposing inflammatory and regulatory roles in a murine model of lupus. *Immunity*. 2006;25(3):417–428.
17. Nickerson KM, Christensen SR, Cullen JL, Meng W, Luning Prak ET, Shlomchik MJ. TLR9 promotes tolerance by restricting survival of anergic anti-DNA B cells, yet is also required for their

activation. *J Immunol*. 2013;190(4):1447–1456.
18. Nickerson KM, et al. TLR9 regulates TLR7- and MyD88-dependent autoantibody production and disease in a murine model of lupus. *J Immunol*. 2010;184(4):1840–1848.
19. Santiago-Raber ML, et al. Critical role of TLR7 in the acceleration of systemic lupus erythematosus in TLR9-deficient mice. *J Autoimmun*. 2010;34(4):339–348.
20. Yu P, et al. Toll-like receptor 9-independent aggravation of glomerulonephritis in a novel model of SLE. *Int Immunol*. 2006;18(8):1211–1219.
21. Cheema GS, Roschke V, Hilbert DM, Stohl W. Elevated serum B lymphocyte stimulator levels in patients with systemic immune-based rheumatic diseases. *Arthritis Rheum*. 2001;44(6):1313–1319.
22. Mariette X, et al. The level of BLyS (BAFF) correlates with the titre of autoantibodies in human Sjögren's syndrome. *Ann Rheum Dis*. 2003;62(2):168–171.
23. Sanz I, Yasothan U, Kirkpatrick P. Belimumab. *Nat Rev Drug Discov*. 2011;10(5):335–336.
24. Stohl W, Scholz JL, Cancro MP. Targeting BLyS in rheumatic disease: the sometimes-bumpy road from bench to bedside. *Curr Opin Rheumatol*. 2011;23(3):305–310.
25. Zhang J, et al. Cutting edge: a role for B lymphocyte stimulator in systemic lupus erythematosus. *J Immunol*. 2001;166(1):6–10.
26. Bubier JA, et al. A critical role for IL-21 receptor signaling in the pathogenesis of systemic lupus erythematosus in BXSB-Yaa mice. *Proc Natl Acad Sci U S A*. 2009;106(5):1518–1523.
27. Ettinger R, Kuchen S, Lipsky PE. The role of IL-21 in regulating B-cell function in health and disease. *Immunol Rev*. 2008;223:60–86.
28. Hu X, Ivashkiv LB. Cross-regulation of signaling pathways by interferon-gamma: implications for immune responses and autoimmune diseases. *Immunity*. 2009;31(4):539–550.
29. Pollard KM, Cauvi DM, Toomey CB, Morris KV, Kono DH. Interferon-γ and systemic autoimmunity. *Discov Med*. 2013;16(87):123–131.
30. Berland R, et al. Toll-like receptor 7-dependent loss of B cell tolerance in pathogenic autoantibody knockin mice. *Immunity*. 2006;25(3):429–440.
31. Kono DH, et al. Endosomal TLR signaling is required for anti-nucleic acid and rheumatoid factor autoantibodies in lupus. *Proc Natl Acad Sci U S A*. 2009;106(29):12061–12066.
32. Lartigue A, et al. Role of TLR9 in anti-nucleosome and anti-DNA antibody production in lpr mutation-induced murine lupus. *J Immunol*. 2006;177(2):1349–1354.
33. Lee PY, et al. TLR7-dependent and Fcgamma R-independent production of type I interferon in experimental mouse lupus. *J Exp Med*. 2008;205(13):2995–3006.
34. Silver KL, Crockford TL, Bouriez-Jones T, Milling S, Lambe T, Cornall RJ. MyD88-dependent autoimmune disease in Lyn-deficient mice. *Eur J Immunol*. 2007;37(10):2734–2743.
35. Naradikian MS, et al. Cutting edge: IL-4, IL-21, and IFN-γ interact to govern T-bet and CD11c expression in TLR-activated B cells. *J Immunol*. 2016;197(4):1023–1028.
36. Rubtsov AV, et al. Toll-like receptor 7 (TLR7)-driven accumulation of a novel CD11c^{+} B-cell population is important for the development of autoimmunity. *Blood*. 2011;118(5):1305–1315.
37. Rubtsov AV, Rubtsova K, Kappler JW, Marrack P. TLR7 drives accumulation of ABCs and autoantibody production in autoimmune-prone mice. *Immunol Res*. 2013;55(1-3):210–216.
38. Leadbetter EA, Rifkin IR, Hohlbaum AM, Beaudette BC, Shlomchik MJ, Marshak-Rothstein A. Chromatin-IgG complexes activate B cells by dual engagement of IgM and Toll-like receptors. *Nature*. 2002;416(6881):603–607.
39. Uccellini MB, et al. Autoreactive B cells discriminate CpG-rich and CpG-poor DNA and this response is modulated by IFN-alpha. *J Immunol*. 2008;181(9):5875–5884.
40. Kaiser WJ, et al. RIP3 mediates the embryonic lethality of caspase-8-deficient mice. *Nature*. 2011;471(7338):368–372.
41. Bossen C, Schneider P. BAFF, APRIL and their receptors: structure, function and signaling. *Semin Immunol*. 2006;18(5):263–275.
42. Hatada EN, et al. NF-kappa B1 p50 is required for BLyS attenuation of apoptosis but dispensable for processing of NF-kappa B2 p100 to p52 in quiescent mature B cells. *J Immunol*. 2003;171(2):761–768.
43. Hsu BL, Harless SM, Lindsley RC, Hilbert DM, Cancro MP. Cutting edge: BLyS enables survival of transitional and mature B cells through distinct mediators. *J Immunol*. 2002;168(12):5993–5996.
44. Treml LS, et al. TLR stimulation modifies BLyS receptor expression in follicular and marginal zone B cells. *J Immunol*. 2007;178(12):7531–7539.
45. Harless SM, et al. Competition for BLyS-mediated signaling through Bcmd/BR3 regulates peripheral B lymphocyte numbers. *Curr Biol*. 2001;11(24):1986–1989.
46. Li X, Jiang S, Tapping RI. Toll-like receptor signaling in cell proliferation and survival. *Cytokine*. 2010;49(1):1–9.
47. Dal Porto JM, Gauld SB, Merrell KT, Mills D, Pugh-Bernard AE, Cambier J. B cell antigen receptor signaling 101. *Mol Immunol*. 2004;41(6-7):599–613.
48. Busconi L, et al. Functional outcome of B cell activation by chromatin immune complex engagement of the B cell receptor and TLR9. *J Immunol*. 2007;179(11):7397–7405.
49. Chaturvedi A, Dorward D, Pierce SK. The B cell receptor governs the subcellular location of Toll-like receptor 9 leading to hyperresponses to DNA-containing antigens. *Immunity*. 2008;28(6):799–809.
50. Ambrosino C, Nebreda AR. Cell cycle regulation by p38 MAP kinases. *Biol Cell*. 2001;93(1–2):47–51.
51. Lopes-Carvalho T, Kearney JF. Marginal zone B cell physiology and disease. *Curr Dir Autoimmun*. 2005;8:91–123.
52. Wardemann H, Yurasov S, Schaefer A, Young JW, Meffre E, Nussenzweig MC. Predominant autoantibody production by early human B cell precursors. *Science*. 2003;301(5638):1374–1377.
53. Chen X, Martin F, Forbush KA, Perlmutter RM, Kearney JF. Evidence for selection of a population of multi-reactive B cells into the splenic marginal zone. *Int Immunol*. 1997;9(1):27–41.
54. Hardy RR, Li YS, Allman D, Asano M, Gui M, Hayakawa K. B-cell commitment, development and selection. *Immunol Rev*. 2000;175:23–32.
55. Cancro MP. Peripheral B-cell maturation: the intersection of selection and homeostasis. *Immunol Rev*. 2004;197:89–101.
56. Meyer-Bahlburg A, Rawlings DJ. Differential impact of Toll-like receptor signaling on distinct B cell subpopulations. *Front Biosci (Landmark Ed)*. 2012;17:1499–1516.
57. Erikson J, Radic MZ, Camper SA, Hardy RR, Carmack C, Weigert M. Expression of anti-DNA immunoglobulin transgenes in non-autoimmune mice. *Nature*. 1991;349(6307):331–334.
58. Gay D, Saunders T, Camper S, Weigert M. Receptor editing: an approach by autoreactive B cells to escape tolerance. *J Exp Med*. 1993;177(4):999–1008.
59. Hondowicz BD, et al. The role of BLyS/BLyS receptors in anti-chromatin B cell regulation. *Int Immunol*. 2007;19(4):465–475.
60. Radic MZ, Erikson J, Litwin S, Weigert M. B lymphocytes may escape tolerance by revising their antigen receptors. *J Exp Med*. 1993;177(4):1165–1173.
61. Di Domizio J, et al. Binding with nucleic acids or glycosaminoglycans converts soluble protein oligomers to amyloid. *J Biol Chem*. 2012;287(1):736–747.
62. Dorta-Estremera SM, Li J, Cao W. Rapid generation of amyloid from native proteins in vitro. *J Vis Exp*. 2013;5(82):50869.
63. Wagner H. The immunogenicity of CpG-antigen conjugates. *Adv Drug Deliv Rev*. 2009;61(3):243–247.
64. Lahoud MH, et al. DEC-205 is a cell surface receptor for CpG oligonucleotides. *Proc Natl Acad Sci U S A*. 2012;109(40):16270–16275.
65. Roberts TL, et al. B cells do not take up bacterial DNA: an essential role for antigen in exposure of DNA to toll-like receptor-9. *Immunol Cell Biol*. 2011;89(4):517–525.
66. Guiducci C, et al. Properties regulating the nature of the plasmacytoid dendritic cell response to Toll-like receptor 9 activation. *J Exp Med*. 2006;203(8):1999–2008.
67. Sasai M, Linehan MM, Iwasaki A. Bifurcation of Toll-like receptor 9 signaling by adaptor protein 3. *Science*. 2010;329(5998):1530–1534.
68. Chaturvedi A, Pierce SK. How location governs toll-like receptor signaling. *Traffic*. 2009;10(6):621–628.
69. De Chiara G, et al. Bcl-2 Phosphorylation by p38 MAPK: identification of target sites and biologic consequences. *J Biol Chem*. 2006;281(30):21353–21361.
70. Cai B, Chang SH, Becker EB, Bonni A, Xia Z. p38 MAP kinase mediates apoptosis through phosphorylation of BimEL at Ser-65. *J Biol Chem*. 2006;281(35):25215–25222.
71. Thornton TM, Rincon M. Non-classical p38 map kinase functions: cell cycle checkpoints and survival. *Int J Biol Sci*. 2009;5(1):44–51.
72. Jackson SW, et al. Opposing impact of B cell-intrinsic TLR7 and TLR9 signals on autoantibody repertoire and systemic inflammation. *J Immunol*. 2014;192(10):4525–4532.
73. Isnardi I, et al. IRAK-4- and MyD88-dependent pathways are essential for the removal of developing autoreactive B cells in humans. *Immunity*. 2008;29(5):746–757.

74. Rubtsova K, Rubtsov AV, Cancro MP, Marrack P. Age-associated B cells: A T-bet-dependent effector with roles in protective and pathogenic immunity. *J Immunol*. 2015;195(5):1933–1937.
75. Nündel K, et al. Cell-intrinsic expression of TLR9 in autoreactive B cells constrains BCR/TLR7-dependent responses. *J Immunol*. 2015;194(6):2504–2512.
76. Green NM, Moody KS, Debatis M, Marshak-Rothstein A. Activation of autoreactive B cells by endogenous TLR7 and TLR3 RNA ligands. *J Biol Chem*. 2012;287(47):39789–39799.
77. Zikherman J, Parameswaran R, Weiss A. Endogenous antigen tunes the responsiveness of naive B cells but not T cells. *Nature*. 2012;489(7414):160–164.
78. von Bülow GU, van Deursen JM, Bram RJ. Regulation of the T-independent humoral response by TACI. *Immunity*. 2001;14(5):573–582.
79. Grillot DA, et al. bcl-x exhibits regulated expression during B cell development and activation and modulates lymphocyte survival in transgenic mice. *J Exp Med*. 1996;183(2):381–391.
80. Goenka R, et al. Local BLyS production by T follicular cells mediates retention of high affinity B cells during affinity maturation. *J Exp Med*. 2014;211(1):45–56.
81. Schmidt AM, et al. Diacylglycerol kinase ζ limits the generation of natural regulatory T cells. *Sci Signal*. 2013;6(303):ra101.
82. Stadanlick JE, et al. Tonic B cell antigen receptor signals supply an NF-kappaB substrate for prosurvival BLyS signaling. *Nat Immunol*. 2008;9(12):1379–1387.
83. Oropallo MA, et al. Chronic spinal cord injury impairs primary antibody responses but spares existing humoral immunity in mice. *J Immunol*. 2012;188(11):5257–5266.
84. Avalos AM, Uccellini MB, Lenert P, Viglianti GA, Marshak-Rothstein A. FcγRIIB regulation of BCR/TLR-dependent autoreactive B-cell responses. *Eur J Immunol*. 2010;40(10):2692–2698.

The Journal of Immunology

Age-Associated B Cells Express a Diverse Repertoire of V_H and Vκ Genes with Somatic Hypermutation

Lisa M. Russell Knode, Martin S. Naradikian, Arpita Myles, Jean L. Scholz, Yi Hao, Danya Liu, Mandy L. Ford, John W. Tobias, Michael P. Cancro and Patricia J. Gearhart

J Immunol 2017; 198:1921-1927; Prepublished online 16 January 2017;
doi: 10.4049/jimmunol.1601106
http://www.jimmunol.org/content/198/5/1921

The Journal of Immunology is published twice each month by The American Association of Immunologists, Inc., 9650 Rockville Pike, Bethesda, MD 20814-3994.

Print ISSN: 0022-1767 Online ISSN: 1550-6606.

Age-Associated B Cells Express a Diverse Repertoire of V_H and Vκ Genes with Somatic Hypermutation

Lisa M. Russell Knode,* Martin S. Naradikian,† Arpita Myles,† Jean L. Scholz,† Yi Hao,†,1 Danya Liu,‡ Mandy L. Ford,‡ John W. Tobias,§ Michael P. Cancro,† and Patricia J. Gearhart*

The origin and nature of age-associated B cells (ABCs) in mice are poorly understood. In this article, we show that their emergence required MHC class II and CD40/CD40L interactions. Young donor B cells were adoptively transferred into congenic recipients and allowed to remain for 1 mo in the absence of external Ag. B cells expressing the T-bet transcription factor, a marker for ABCs, were generated after multiple cell divisions from C57BL/6 donors but not from MHC class II– or CD40-deficient donors. Furthermore, old CD154 (CD40L)-deficient mice did not accrue ABCs, confirming that they arise primarily through T-dependent interactions. To determine what Igs ABCs express, we sequenced V_H and Vκ rearranged genes from unimmunized 22-mo-old C57BL/6 mice and showed that they had a heterogeneous repertoire, which was comparable to that seen in old follicular and marginal zone B cell subsets. However, in contrast to the follicular and marginal zone cells, ABCs displayed significant somatic hypermutation. The mutation frequency was lower than found in germinal center cells after deliberate immunization, suggesting that ABCs have undergone mild stimulation from endogenous Ags over time. These observations show that quiescent ABCs are Ag-experienced cells that accumulate during T cell–dependent responses to diverse Ags during the life of an individual. ***The Journal of Immunology*****, 2017, 198: 1921–1927.**

Profound changes in the composition and dynamics of lymphoid populations occur with age, likely contributing to the decline in immune status, collectively termed immune senescence. For example, B cell production from bone marrow steadily decreases with age, yet the numbers of peripheral B cells remain relatively constant as a result of slowed turnover and altered representation of naive and Ag-experienced B cell subsets (1–8). A novel B cell subset that accumulates with age, termed age-associated B cells (ABCs), was identified recently (9–12). These cells have unique features that include preferential responsiveness to TLR7 and TLR9 ligands, surface markers consistent with prior Ag activation, and expression of the T-box transcription factor, Tbx21 (T-bet), which is required for their accumulation (13). Some ABCs also express Itgax (CD11c), an integrin that potentiates their ability to present Ag to T cells (14). ABCs are associated with the onset and severity of humoral autoimmunity in animal models and humans (10, 15, 16). Further, these cells play roles in age-associated immune dysfunctions, including elevated inflammatory cytokine levels and reduced B cell generation rates (11). Finally, a growing literature suggests that B cells with similar characteristics arise during some viral, bacterial, and parasitic infections (13, 17–21), implying a role for ABCs in normal immune function.

Despite these observations, the origin and nature of ABCs remain poorly understood. In this study, we investigated their formation, Ig repertoire, and level of somatic hypermutation. The results indicate a polyclonal, Ag-experienced B cell population that arises primarily through T-dependent immune responses to diverse endogenous Ags.

Materials and Methods

Mice

All mice used for experiments were females on a C57BL/6 background. Old mice were obtained from the Charles River aged mouse colony at 18 mo of age and used at 22 mo. *Cd154*$^{-/-}$ (B6.129S2-Cd40lg^{tm1Imx}/J) mice were purchased from the Jackson Laboratory and kept until 22 mo of age. Young (2–4 mo) CD45.1 and CD45.2 mice were obtained from the Jackson Laboratory. Young *I-Ab*$^{-/-}$ mice were from Terri Laufer (University of Pennsylvania), and *Cd40*$^{-/-}$ spleens from young mice were sent from M. Ford's colony. *Aid*$^{-/-}$ mice were bred in the National Institute on Aging colony. Animal protocols were reviewed and approved by the Animal Care and Use Committees at the National Institute on Aging and the University of Pennsylvania.

Adoptive transfers

CD23$^+$ splenic B cells from 2-mo-old CD45.2 mice were enriched by positive selection using the MACS bead system (Miltenyi Biotec). Cells

*Laboratory of Molecular Biology and Immunology, National Institute on Aging, National Institutes of Health, Baltimore, MD 21224; †Department of Pathology and Laboratory Medicine, Perelman School of Medicine, University of Pennsylvania, Philadelphia, PA 19104; ‡Emory Transplant Center and Department of Surgery, Emory University, Atlanta, GA 30322; and §Penn Molecular Profiling Facility, Perelman School of Medicine, University of Pennsylvania, Philadelphia, PA 19104

[1]Current address: Tongji Medical College, Wuhan, China.

ORCIDs: 0000-0003-1926-0382 (M.S.N.); 0000-0001-6103-6486 (D.L.); 0000-0002-5362-7013 (J.W.T.); 0000-0003-1975-4737 (P.J.G.).

Received for publication June 24, 2016. Accepted for publication December 20, 2016.

This work was supported by the Intramural Research Program of the National Institutes of Health, National Institute on Aging (to L.M.R.K. and P.J.G.) and by Grants PR130769 (Department of the Army) and R01 AG030227 (National Institute on Aging) (to M.P.C.). M.S.N. was supported in part by National Institute of Allergy and Infectious Diseases Grant T32 AI055428.

L.M.R.K., M.S.N., M.P.C., and P.J.G. designed experiments; L.M.R.K., M.S.N., A.M., Y.H., J.L.S., and J.W.T. performed research and analyzed data; D.L. and M.L.F. contributed reagents; and L.M.R.K., M.S.N., J.L.S, J.W.T., M.P.C., and P.J.G. wrote the manuscript.

Address correspondence and reprint requests to Dr. Michael P. Cancro or Dr. Patricia J. Gearhart, Department of Pathology and Laboratory Medicine, 284 John Morgan Building, 3620 Hamilton Walk, University of Pennsylvania, Philadelphia, PA 19104 (M.P.C.) or Laboratory of Molecular Biology and Immunology, National Institute on Aging, National Institutes of Health, 251 Bayview Boulevard, Baltimore, MD 21224 (P.J.G.). E-mail addresses: cancro@mail.med.upenn.edu (M.P.C.) or gearhartp@mail.nih.gov (P.J.G.)

The online version of this article contains supplemental material.

Abbreviations used in this article: ABC, age-associated B cell; AID, activation-induced deaminase; FO, follicular; HA, hemagglutinin; HA-PE, PE-labeled probe that recognizes HA of PR8; MZ, marginal zone; PR8, influenza strain A/Puerto Rico/8/1934.

were labeled with CFSE (eBioscience), according to the manufacturer's instructions, and 8 million cells were transferred into each CD45.1 congenic host by retro-orbital injection.

Flow cytometry and FACS sorting

Single-cell suspensions were prepared from spleens and stained with fluorochrome-conjugated Abs. For flow cytometry of the adoptive-transfer and influenza experiments, we used Live/Dead Zombie Aqua, anti-CD45.1-AF700 (A20), anti-CD45.2-BV421 (104), anti-CD19-BV785 (6D5), anti-CD23 biotin (B3B4), and anti-CD11c (N418) (BioLegend). Anti-CD43–PE (S7) was from BD Biosciences. Cells were analyzed on an LSRII, and data were analyzed using FlowJo software (TreeStar). Intracellular stains for T-bet were performed with anti–T-bet–allophycocyanin (4B10; BioLegend) and a Foxp3 transcription factor kit (eBioscience), according to the manufacturer's instructions. For FACS sorting to isolate subsets, we used anti-CD43–allophycocyanin (S7; BD Biosciences). Anti-CD23–PE Cy7 (B3B4), anti-CD21/CD35–eFluor 450 (4E3), anti-CD45R–FITC (B220, RA3-6B2), and anti-CD93 (AA4.1)-allophycocyanin were from eBioscience. Stained splenocytes were analyzed with a BD FACSCanto II or sorted using a BD FACSAria III, BD FACSAria Fusion, iCyt Reflection (Sony Biotechnology), or Beckman Coulter MoFlo. Follicular (FO) B cells were isolated as CD93 (AA4.1)$^-$ CD43$^-$ B220$^+$ CD21/35$^+$ CD23$^+$. Marginal zone (MZ) B cells were isolated as CD93 (AA4.1)$^-$ CD43$^-$ B220$^+$ CD21/35$^+$ CD23^{lo}. ABCs were isolated as CD93 (AA4.1)$^-$ CD43$^-$ B220$^+$ CD21/35$^-$ CD23$^-$. Analyses were done using FlowJo software.

V gene identification and mutation analyses

Sorted cells were lysed in TRIzol reagent, and RNA was prepared. cDNA was synthesized using SuperScript III Reverse Transcriptase (Invitrogen). Ig H chain VDJ genes and Ig κ light (Igκ)-chain VJ genes were amplified using Taq polymerase (TaKaRa; Clontech) with 5′ degenerate primers specific to framework 1 of V genes and 3′ primers located in IgM or Igκ constant regions, as previously described (22). PCR products were cloned into StrataClone TA cloning vector (Agilent Technologies) and sequenced. Only sequences with unique VDJ or VJ joins were counted. The sequences were blasted against the mouse Ig loci using IgBLAST from the National Center for Biotechnology Information to identify V, D, and J gene segment usage and mutations. For mutational analysis of the J_H4 intron, DNA was prepared, and a 492-bp intronic region downstream of J_H4 from rearranged V_HJ558 genes was amplified using nested PCR. The first round used forward primer J558 5′-AGCCTGACATCTGAGGAC-3′ and reverse primer V1.8NR4R 5′-TCCATACACATACTTCTGTGTTCCT-3′, and the second round used the same J558 forward primer listed above and reverse primer JH2827Bam 5′-CGCGGATCCGATGCCTTTCTCCCTTGACTC-3′. DNA was amplified using Herculase II Fusion DNA Polymerase (Agilent Technologies). The amplified PCR products were cloned into a StrataClone Blunt PCR Cloning vector (Agilent Technologies) and sequenced.

Influenza virus infection and analysis

Four-month-old C57BL/6 mice were left uninfected or infected intranasally with 30 tissue culture infectious $dose_{50}$ of influenza strain A/Puerto Rico/8/1934 (PR8), which was provided by Dr. S. Hensley (University of Pennsylvania). Both uninfected and infected mice were sacrificed 100 d later. To detect hemagglutinin (HA)-reactive B cells, we used a PE-labeled probe that recognizes HA of PR8 (HA-PE) (23). The probe was used at a concentration of 1:500, and data acquisition and analysis were performed as described (23).

Results

ABC generation requires B cell expression of MHC class II and CD40

We showed previously that ABCs could arise from FO B cells after in vivo expansion in adoptive hosts (9). This extensive division may reflect homeostatic expansion or could implicate Ag-driven activation involving T cell help and costimulation. To distinguish between these possibilities, we modified our adoptive-transfer model with CFSE-labeled donor B cells to use MHC class II– or CD40-deficient donor B cells. The rationale was that homeostatic expansion should be independent of Ag presentation and costimulation, whereas Ag-driven events should not. As shown in Fig. 1A, after 1 mo in the absence of immunization, a small proportion (~0.2%) of C57BL/6 donor B cells underwent five to eight rounds of division, likely in response to stimulation by endogenous Ags. These extensively divided CFSE^{lo} cells were CD23$^-$ and T-bet$^+$, which are markers for ABCs. Although the events occurred in only a month, they represent a snapshot of the slow accumulation of ABCs with time. In contrast, B cells from MHC class II–deficient (*I-Ab*$^{-/-}$) and CD40-deficient (*Cd40*$^{-/-}$) mice underwent fewer divisions with far less T-bet expression than

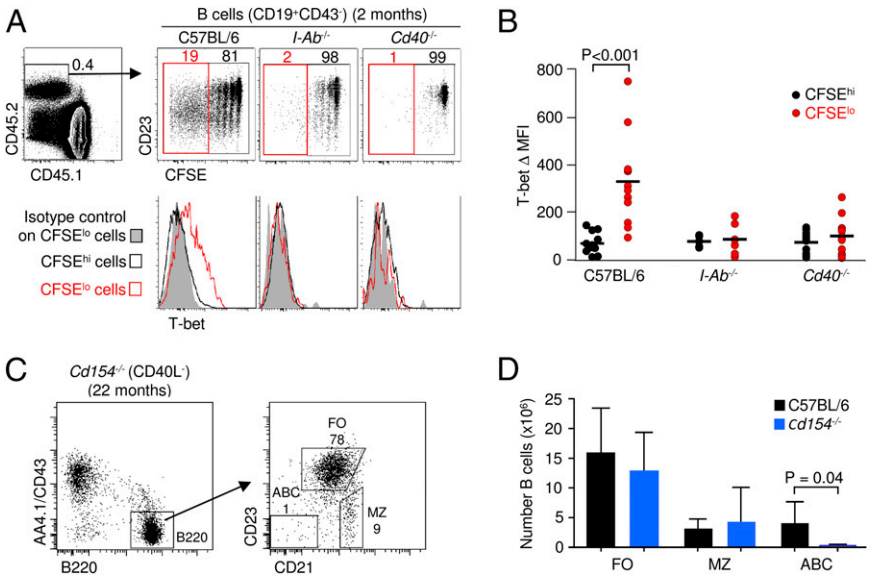

FIGURE 1. Interactions with MHC class II and CD40 drive the accumulation of ABCs. (**A**) CD23$^+$ FO B cells from 2-mo-old donor mice (CD45.2) were labeled with CFSE and adoptively transferred into young congenic CD45.1 hosts. Recipient mice were analyzed 1 mo later. Shown are a representative plot of the gating strategy and representative dot plots of CFSE dilution in C57BL/6, *I-Ab*$^{-/-}$, and *Cd40*$^{-/-}$ cells. Numbers depict the percentage of cells in each box. Cells with multiple rounds of proliferation (CFSE^{lo}) are boxed in red. Line graphs show intracellular staining for T-bet in CFSE^{lo} cells. (**B**) Analyses of T-bet change in mean fluorescence intensity (ΔMFI) are summarized in three independent experiments for a total of 12 mice for C57BL/6, 6 mice for *I-Ab*$^{-/-}$, and 12 mice for *Cd40*$^{-/-}$. (**C**) Spleen cells from 22-mo-old *Cd154*$^{-/-}$ mice were gated on live B220$^+$ cells. A representative dot plot shows the absence of ABCs (CD23$^-$CD21$^-$). Numbers represent the percentage of B cells in each population. (**D**) Absolute B cell numbers of the indicated cell subset from old C57BL/6 and *Cd154*$^{-/-}$ mice. Error bars signify the SD of values from 31 C57BL/6 mice and 5 *Cd154*$^{-/-}$ mice. The *p* values were calculated by an unpaired, equal variance Student *t* test.

did C57BL/6 cells of the same division cohort. Analyses of multiple mice (Fig. 1B) confirmed a significant increase in T-bet mean fluorescence intensity in $CFSE^{lo}$ cells compared with $CFSE^{hi}$ cells from C57BL/6 donors, whereas cells from *I-Ab*$^{-/-}$ and *Cd40*$^{-/-}$ donors had no increase. The data suggest that ABCs arise from B cells involved in immune responses to T-dependent Ags, because cognate Ag-presenting capacity and competence to receive CD40 costimulation are required. This interpretation further predicts that CD154-deficient mice, which lack CD40L, should have reduced ABC accumulation. Consistent with this expectation, analysis of splenic B cells from 22-mo-old CD154-deficient mice revealed a paucity of ABCs (Fig. 1C), despite no change in FO and MZ compartments compared with controls (Fig. 1D). Collectively, these results show that ABCs are generated slowly after endogenous Ag presentation via MHC class II and costimulation via the CD40 receptor with CD40L on T cells. The notion that ABCs are derived from T-dependent immune responses raises questions about the breadth and nature of potential Ags involved in their generation and whether they bear hallmarks of germinal center participation. Accordingly, we interrogated Ig variable (V) gene usage and levels of somatic hypermutation among quiescent, naturally occurring ABCs from old mice.

ABCs exhibit a diverse V gene segment repertoire

ABC accumulation may reflect the aggregate of immune responses to a large and diverse class of endogenous Ags and, thus, involve a broad array of clonotypic specificities. Alternatively, accumulation could be mediated by common exposure to a limited array of self- or environmental ligands that generate oligoclonal expansions with limited repertoire diversity. To differentiate between these possibilities, we sorted FO, MZ, and ABC B cell subsets from 22-mo-old mice and compared V_H and Vκ gene segment usage. Because the majority of ABCs express IgM (9), sequencing analyses for H chain genes were done on cDNA amplified with a Cμ 3′ primer and degenerate V_H 5′ primers. Likewise, κ L chain genes were identified by amplifying cDNA with a Cκ 3′ primer and degenerate Vκ 5′ primers. Some 2400 unique sequences for both loci were collected and analyzed. Overall, the usage of V_H and Vκ gene segments was similar among all three subsets. For V_H genes, 85 genes from 12 families were identified, and their frequencies were measured within the subsets. ABCs were compared separately with FO (Fig. 2A) and MZ (Fig. 2B) cells, and significant differences in over- or underutilization were seen in only two to four individual genes. For Vκ genes, 69 genes from 15 families were found; when ABCs were compared with FO (Fig. 3A) or MZ (Fig. 3B) cells, only three to five genes were significantly over- or underused. Thus, there was no evidence for strong repertoire skewing, arguing against a restricted Ag-driven response. We also did not observe significant selection for amino acid replacement changes in CDRs for Ig H chain and Igκ-chains from the ABC population (data not shown). These results suggest that ABCs develop in response to a broad range of Ags.

ABC V genes have undergone somatic hypermutation

The requirement for CD40–CD154 interactions in ABC accumulation suggests that most ABCs are products of activation involving cognate T cell help. If so, the V genes of ABCs should contain increased frequencies of mutations compared with other subsets. To

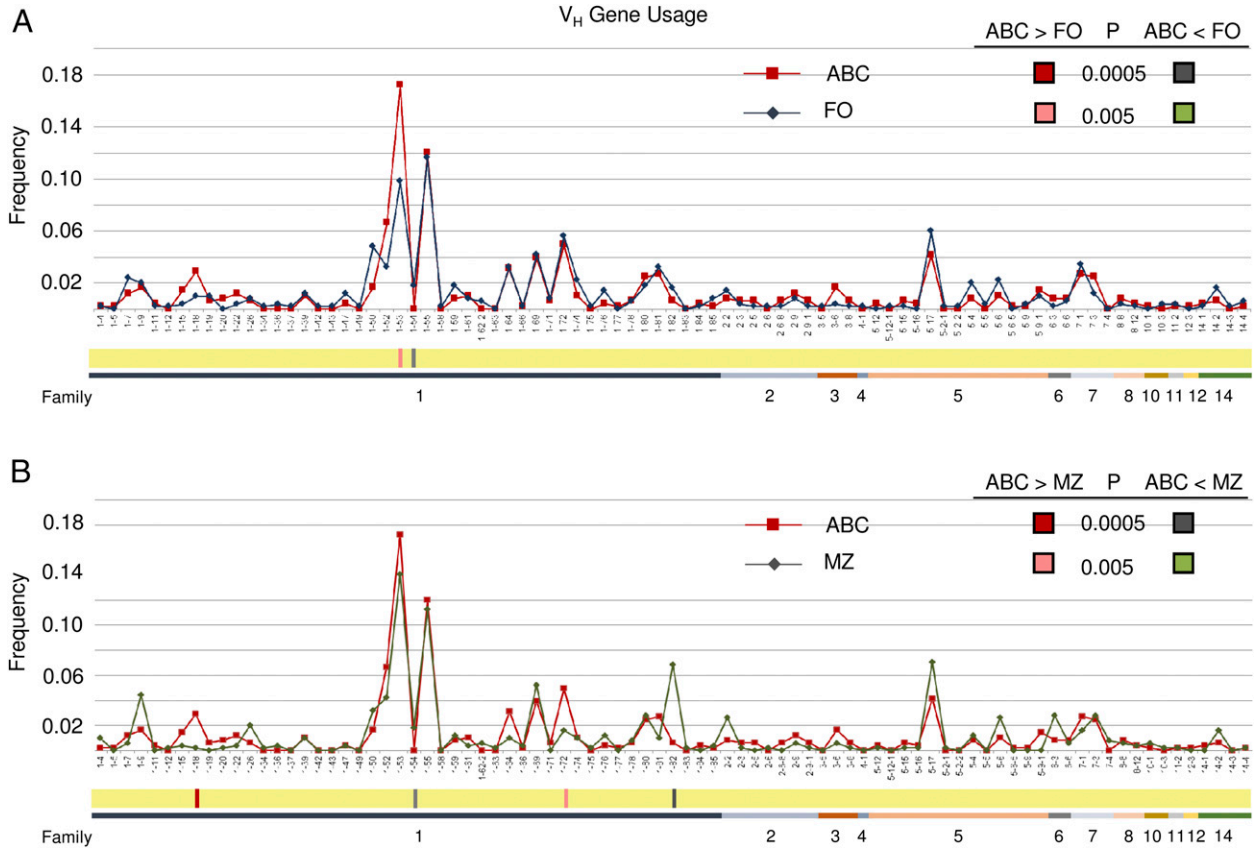

FIGURE 2. Diverse V_H gene segment usage in ABCs. The frequency of gene expression within the indicated B cell population in old mice (n = 18–24 mice for FO, MZ, and ABC subsets) was determined using RT-PCR. For each subset, ~400 V_H sequences were analyzed. V genes were grouped by family, which is indicated numerically below the graph. Significant differences in V gene usage between ABC and FO (**A**) or between ABC and MZ (**B**) subsets were calculated using the Fisher exact test and are shown below the gene name in the yellow bar. The p value heat map scale is shown.

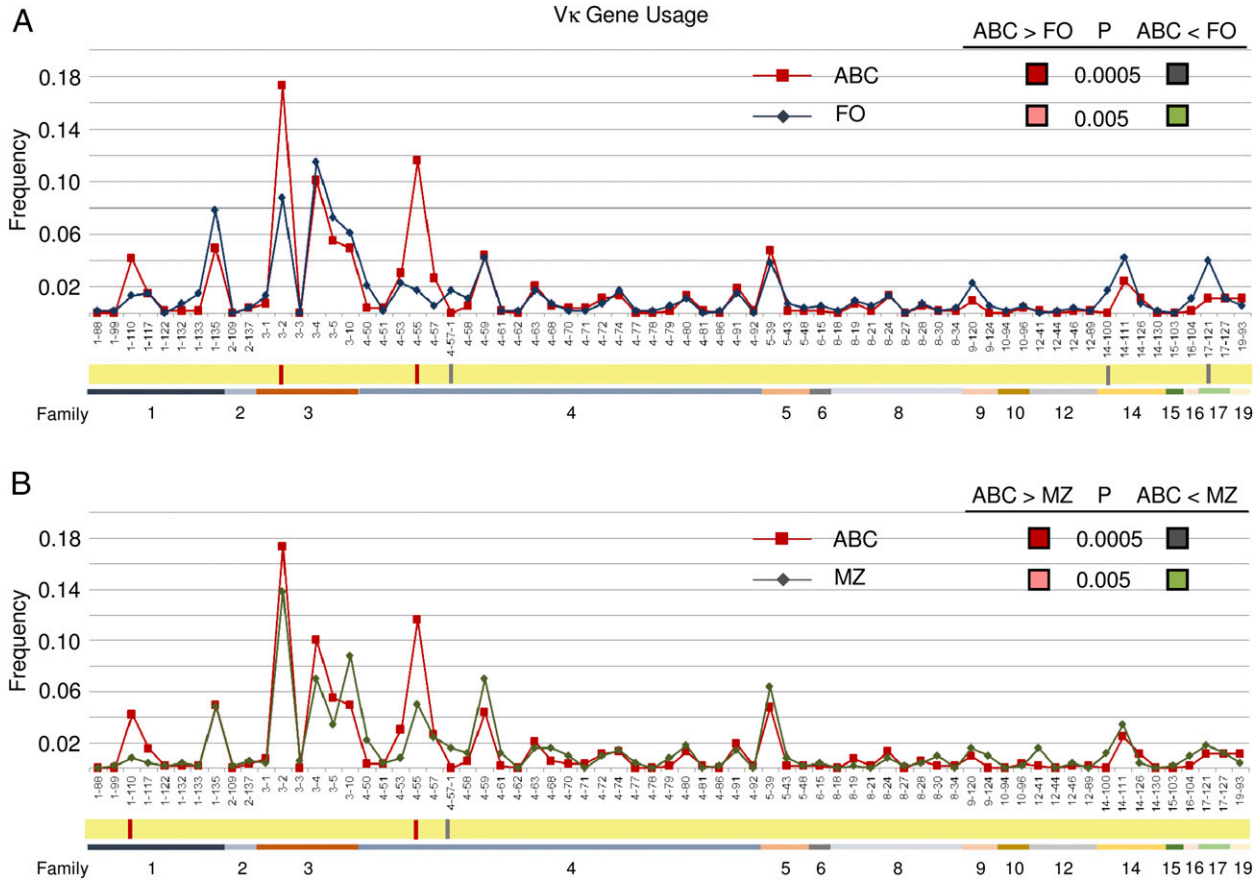

FIGURE 3. Diverse Vκ gene segment usage in ABCs. (**A**) ABC vs. FO subsets. (**B**) ABC vs. MZ subsets. Details are similar to Fig. 2 legend.

address this, we counted the number of mutations in VDJ heavy and VJ κ light exons amplified from FO, MZ, and ABC B cell subsets from 22-mo-old mice used for the repertoire analysis. Sequences of V, D, and J gene segments were compared with their germline counterparts to identify mutations. VDJ and VJ genes from ABCs had a significant 4-fold increase in mutations compared with FO cells and a significant 2-fold increase compared with MZ cells (Fig. 4A, 4B). As a control, V exons were sequenced from FO and MZ cells from young *Aid*$^{-/-}$ mice, which cannot undergo hypermutation because the activation-induced deaminase protein is absent. The mutation frequency was $\sim 2 \times 10^{-3}$ mutations per base pair for activation-induced deaminase–deficient cells, which represents the background frequency of errors produced during cDNA synthesis and PCR amplification. The distribution of mutations per sequence is shown in Fig. 4C, which shows that two thirds of sequences from ABCs had mutations, indicating that most of these B cells have encountered some type of Ag during their existence. An examination of the types of nucleotide substitutions in the cadre of >2700 mutations from VDJ and VJ genes from the ABC sequences showed no difference compared with FO and MZ substitutions (data not shown). Because the error rate for sequencing cDNA clones from RNA is elevated due to errors from the low-fidelity reverse transcriptase used to make cDNA, we also analyzed mutations in the 492-bp J_H4 intronic region directly from DNA, using a high-fidelity polymerase. FO, MZ, and ABC B cell subsets were sorted as described above, and the J_H4 region was amplified from genomic DNA. As shown in Fig. 4D–F, there was a significant increase in mutation frequency from ABCs compared with those from FO and MZ cells, confirming that ABCs have undergone somatic hypermutation. As a control, introns were sequenced from germinal center B cells of young mice taken 4 wk after immunization with (4-hydroxy-3-nitrophenyl) acetyl–chicken γ globulin (24), and the frequency was 5-fold higher than in ABCs. This comparison places ABCs in the middle between naive and germinal center cells, suggesting that they undergo mild chronic stimulation by endogenous Ags versus acute stimulation by immunization.

Some Ag-specific B cells express T-bet and CD11c

Our results suggest an Ag-driven origin for ABCs that, coupled with their continuous accumulation, BLyS independence, and resting state (9, 25), lends credence to the idea that they are an unusual subset of B cells. To further interrogate the provenance of ABCs, we compared their gene-expression profiles with those from FO B cells sorted from old and young mice. ABC uniqueness is shown by a subset of 70 genes with ≥5-fold higher expression in old ABCs compared with old and young FO B cells (Supplemental Fig. 1A, Supplemental Table I). T-bet and CD11c were overexpressed in ABCs, confirming previous reports (13, 14). Principal component analysis was used to visualize intersample variation among all of the genes from sorted subsets and illustrated that old ABCs have distinct gene-expression profiles compared with FO B cells from old and young mice (Supplemental Fig. 1B).

Based on their accumulation of somatic hypermutation, we hypothesized that ABCs represent a subset of Ag-experienced B cells whose accretion reflects the cumulative aggregate of challenges that drive their formation. To demonstrate that another subset of Ag-experienced B cells arising from deliberate infection also expresses T-bet and CD11c, we infected young mice with influenza. HA-specific B cells were tracked by binding to fluorescent labeled HA-PE. Prior to infection, the frequency of HA-reactive B cells was low (Fig. 5A), consistent with prior estimates of ~1/50,000 splenic B cells (26). Following infection, mice displayed the expected

A

Cell type	Sequences	Nucleotides	Mutations	Frequency x 10^{-3}
VDJ exon				
FO	476	139,944	430	3.1
MZ	419	121,929	703	5.8
ABC	372	108,624	1,443	13.3
VJ exon				
FO	460	132,940	419	3.2
MZ	395	112,575	872	7.7
ABC	340	98,600	1,296	13.1

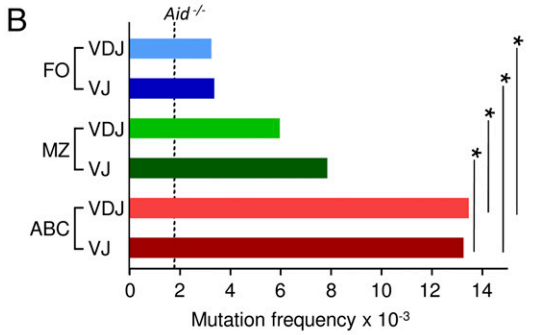

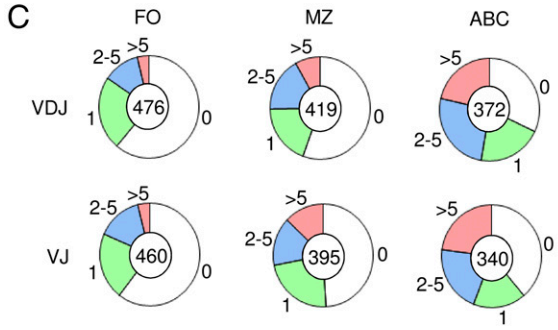

D

Cell type	Sequences	Nucleotides	Mutations	Frequency x 10^{-3}
J_H4 intron				
FO	301	147,791	65	0.4
MZ	301	147,791	90	0.6
ABC	294	144,354	218	1.5

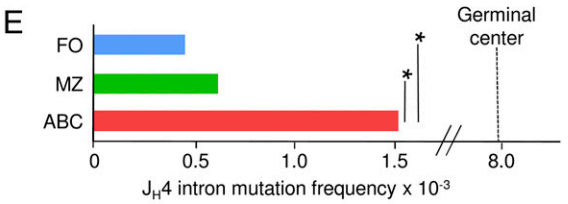

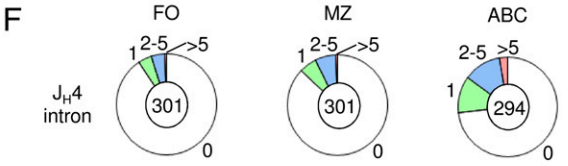

FIGURE 4. ABCs have increased somatic hypermutation. (**A**–**C**) Exon sequences from Figs. 2 and 3 were analyzed for mutations in rearranged VDJ genes for the H chain and in rearranged VJ genes for the κ L chain. (A) Numbers of unique sequences, nucleotides, mutations, and frequencies. (B) Mean mutation frequencies (mutations/nucleotides) in the exons of each B cell subset were calculated. The dotted line indicates the mutation frequency in *Aid*$^{-/-}$ FO and MZ B cells from young mice. (C) Distribution of mutations per sequence. The number of sequences is shown in the center of each circle. Segments represent the proportion of sequences that contain the indicated number of mutations. (**D**–**F**) J_H4 intron sequences were analyzed from genomic DNA of 11–13 mice for each subset. (D). Numbers of sequences, nucleotides, mutations, and frequencies. (E) Mean mutation frequencies; the dotted line represents the frequency in germinal centers from young immunized mice. (F) Distribution of mutations per sequence. *$p < 0.0001$, χ^2 test.

weight loss and fully recovered 30 d later (Fig. 5B), indicating that the virus was cleared. At day 100 postinfection, HA-reactive B cells increased, and ~25% of these were T-bet$^+$CD11c$^+$ (Fig. 5C, 5D). Collectively, these observations on influenza-infected mice support the analogy that some long-lived Ag-experienced cells express the phenotype associated with ABCs.

Discussion

These studies probe the origin and nature of ABCs, a B cell subset that steadily accumulates with age and whose surface phenotype and transcriptional signature were associated with humoral autoimmunity and antipathogen immune responses. We provide three lines of evidence that ABCs are a unique B cell subset. First, adoptive-transfer studies using MHC class II and CD40-deficient cells confirm our prior report that young FO B cells can give rise to ABCs after extensive division (9) and extend this observation in several ways. Notably, they demonstrate that ABCs can be generated with cognate T cell help, which is substantiated by the lack of ABCs in old *CD154*$^{-/-}$ mice. These findings also significantly connect T-bet expression with these extensively divided cells, a feature that is well established in ABC genesis (12, 13). In addition, our results indicate that homeostatic expansion is unlikely to be the major source of ABCs. The transfer experiments involved replete hosts, with minimal space for donor cells to fill by division, and the relatively few transferred cells from MHC class II– and CD40-deficient donors that divided did not express T-bet. Overall, our data support the hypothesis that most ABCs are the cumulative result of enduring environmental Ag stimulation through T-dependent mechanisms. However, the results do not exclude a TLR-mediated origin for some ABCs that may respond to viral or autoimmune stimuli (27).

Second, analyses of V gene segment use and somatic hypermutation indicate encounters with multiple Ags. The breadth of V-gene usage speaks against a monolithic origin in terms of Ag or epitope recognition and demonstrates that ABCs represent a cross-section of responses to a broad array of Ags. Numerous early reports suggested that the total B cell repertoire was restricted in old mice (5, 28–31). However, our extensive analysis of 85 V_H gene segments and 69 Vκ gene segments revealed a rich spectrum of V-gene usage by FO, MZ, and ABCs from old mice, indicating that global sequencing generates a more comprehensive view of the repertoire than do limited studies of Ag-specific cells. Only a handful of genes were over- or underused by ABCs; overall, there was no significant difference when ABCs were compared with FO

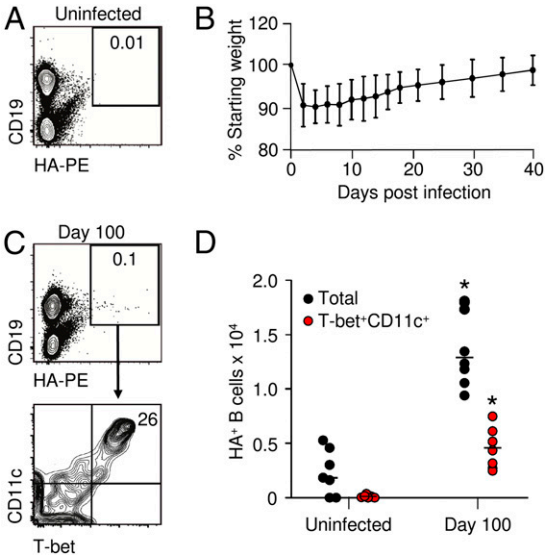

FIGURE 5. B cells infected with influenza HA express T-bet and CD11c. Mice were infected intranasally with PR8, and spleens were harvested 100 d postinfection. (**A**) Representative profile of HA-PE–binding B cells ($CD19^+$) in an uninfected spleen. Number shows the percentage of cells in highlighted box. (**B**) Weight loss and recovery postinfection. Error bars signify SD from eight mice. (**C**) Gating profile for HA-binding B cells in spleens at day 100 (upper panel). Number in box reflects the percentage of cells. A portion of HA-binding B cells express T-bet and CD11c (lower panel). (**D**) Number of B cells that bind HA. Total $T\text{-}bet^-CD11c^-$ and $T\text{-}bet^+CD11c^+$ cells (black circles) compared with only $T\text{-}bet^+CD11c^+$ cells (red circles). Data are from seven uninfected and eight d-100 infected mice collected in three independent experiments. $*p < 0.01$, uninfected versus infected groups, unpaired equal-variance Student *t* test.

or MZ repertoires. Such results would be expected if multiple heterogeneous Ags generated the diverse repertoire. Possible candidates are self-antigens or Ags of the microbiota environment. With regard to self-antigens, a previous report found that mice stimulated chronically with TLR7 agonists developed ABCs expressing high titers of anti-Smith autoimmune Abs (10). However, the few genes that were overused in ABCs in this study did not possess positively charged CDR3 regions in their rearranged sequences, which are common in self-reactive Abs (32). It appears that healthy old mice without deliberate immunization develop a heterogeneous repertoire, without propensity for autoimmune Abs. Although the repertoires of ABCs, FO cells, and MZ cells were similar, the results of the mutation analyses were strikingly different. ABCs showed clear evidence of mutation in the V_H and Vκ exons compared with FO and MZ B cells. Although FO B cells had the lowest mutation frequency, consistent with their preimmune status, the frequency was 2-fold higher in MZ cells, which have likely encountered microbial Ags during circulation, and 4-fold higher in ABCs. In ABCs, mutations did not accumulate in CDRs, consistent with the lack of selection of certain V genes in the repertoire analysis. Furthermore, there was a significant increase in mutation frequency in ABCs in the noncoding J_H4 intron, which is a broad substrate for hypermutation in the absence of selection (33). However, it remains uncertain whether all ABCs are the products of germinal center reactions. For example, most ABCs have IgM receptors and continue to express the surface receptor TACI (9), both of which are inconsistent with the germinal center B cell phenotypes (34). Moreover, the mutation frequency in ABCs was lower compared with germinal center B cells from immunized mice (24). There is precedent for mutated IgM-bearing cells occurring in the absence of germinal centers (35, 36). Alternatively, ABCs may represent early germinal center emigrants that exit before concerted selection (37, 38).

Third, microarray analyses of gene expression show that ABCs from old mice are unique in relation to FO cells from young and old mice. Transcription analysis was also performed by Rubtsov et al. (10) to compare old ABCs with old FO, old B1, and young B1 cells. However, the two analyses profile different sets of genes because the cells were isolated under different conditions. The ABCs in the study from Rubtsov et al. (10) were sorted for $CD11b^+$ expression, and the ABCs analyzed in this study were sorted as $CD21^-$ $CD23^-$. Nonetheless, both analyses show that T-bet and CD11c are greatly increased in old ABCs relative to old FO cells. We found that this signature was also present in some long-lived B cells following influenza infection 100 d later, confirming our previous report (39). By analogy, ABCs are Ag experienced, because they have increased somatic hypermutation, and they require T cell interactions for their generation. The cells presumably arise from chronic stimulation by endogenous Ags, but it is important to note that ABCs are resting cells that persist over time. Whether they can undergo recall responses when they encounter cognate Ags remains to be determined.

Acknowledgments

We thank Robert Maul, Ranjan Sen, and Diana Castiblanco for stimulating conversations and advice, William Yang for technical assistance, and Kate Turlington, Haleigh Larson, and Arielle Kilner for experiments. Robert Wersto, Jade Scheers, Tonya Wallace, and Cuong Nguyen (National Institute on Aging Flow Cytometry Core Facility) assisted in cell sorting. Michael Paley and E. John Wherry (University of Pennsylvania) assisted with the ABC/FO microarray and initial analyses.

Disclosures

The authors have no financial conflicts of interest.

References

1. Miller, J. P., and D. Allman. 2003. The decline in B lymphopoiesis in aged mice reflects loss of very early B-lineage precursors. *J. Immunol.* 171: 2326–2330.
2. Cancro, M. P. 2005. B cells and aging: gauging the interplay of generative, selective, and homeostatic events. *Immunol. Rev.* 205: 48–59.
3. Miller, J. P., and M. P. Cancro. 2007. B cells and aging: balancing the homeostatic equation. *Exp. Gerontol.* 42: 396–399.
4. Kline, G. H., T. A. Hayden, and N. R. Klinman. 1999. B cell maintenance in aged mice reflects both increased B cell longevity and decreased B cell generation. *J. Immunol.* 162: 3342–3349.
5. Johnson, S. A., S. J. Rozzo, and J. C. Cambier. 2002. Aging-dependent exclusion of antigen-inexperienced cells from the peripheral B cell repertoire. *J. Immunol.* 168: 5014–5023.
6. Zheng, B., S. Han, Y. Takahashi, and G. Kelsoe. 1997. Immunosenescence and germinal center reaction. *Immunol. Rev.* 160: 63–77.
7. Frasca, D., and B. B. Blomberg. 2011. Aging impairs murine B cell differentiation and function in primary and secondary lymphoid tissues. *Aging Dis.* 2: 361–373.
8. Goenka, R., J. L. Scholz, M. S. Naradikian, and M. P. Cancro. 2014. Memory B cells form in aged mice despite impaired affinity maturation and germinal center kinetics. *Exp. Gerontol.* 54: 109–115.
9. Hao, Y., P. O'Neill, M. S. Naradikian, J. L. Scholz, and M. P. Cancro. 2011. A B-cell subset uniquely responsive to innate stimuli accumulates in aged mice. *Blood* 118: 1294–1304.
10. Rubtsov, A. V., K. Rubtsova, A. Fischer, R. T. Meehan, J. Z. Gillis, J. W. Kappler, and P. Marrack. 2011. Toll-like receptor 7 (TLR7)-driven accumulation of a novel $CD11c^+$ B-cell population is important for the development of autoimmunity. *Blood* 118: 1305–1315.
11. Ratliff, M., S. Alter, D. Frasca, B. B. Blomberg, and R. L. Riley. 2013. In senescence, age-associated B cells secrete TNFα and inhibit survival of B-cell precursors. *Aging Cell* 12: 303–311.
12. Rubtsova, K., A. V. Rubtsov, M. P. Cancro, and P. Marrack. 2015. Age-associated B cells: a T-bet-dependent effector with roles in protective and pathogenic immunity. *J. Immunol.* 195: 1933–1937.
13. Rubtsova, K., A. V. Rubtsov, L. F. van Dyk, J. W. Kappler, and P. Marrack. 2013. T-box transcription factor T-bet, a key player in a unique type of B-cell activation essential for effective viral clearance. *Proc. Natl. Acad. Sci. USA* 110: E3216–E3224.
14. Rubtsov, A. V., K. Rubtsova, J. W. Kappler, J. Jacobelli, R. S. Friedman, and P. Marrack. 2015. CD11c-expressing B cells are located at the T cell/B cell border in spleen and are potent APCs. *J. Immunol.* 195: 71–79.

15. Ratliff, M., S. Alter, K. McAvoy, D. Frasca, J. A. Wright, S. S. Zinkel, W. N. Khan, B. B. Blomberg, and R. L. Riley. 2015. In aged mice, low surrogate light chain promotes pro-B-cell apoptotic resistance, compromises the PreBCR checkpoint, and favors generation of autoreactive, phosphorylcholine-specific B cells. *Aging Cell* 14: 382–390.
16. Claes, N., J. Fraussen, M. Vanheusden, N. Hellings, P. Stinissen, B. Van Wijmeersch, R. Hupperts, and V. Somers. 2016. Age-associated B cells with proinflammatory characteristics are expanded in a proportion of multiple sclerosis patients. *J. Immunol.* 197: 4576–4583.
17. Moir, S., J. Ho, A. Malaspina, W. Wang, A. C. DiPoto, M. A. O'Shea, G. Roby, S. Kottilil, J. Arthos, M. A. Proschan, et al. 2008. Evidence for HIV-associated B cell exhaustion in a dysfunctional memory B cell compartment in HIV-infected viremic individuals. *J. Exp. Med.* 205: 1797–1805.
18. Weiss, G. E., P. D. Crompton, S. Li, L. A. Walsh, S. Moir, B. Traore, K. Kayentao, A. Ongoiba, O. K. Doumbo, and S. K. Pierce. 2009. Atypical memory B cells are greatly expanded in individuals living in a malaria-endemic area. *J. Immunol.* 183: 2176–2182.
19. Zinöcker, S., C. E. Schindler, J. Skinner, T. Rogosch, M. Waisberg, J. N. Schickel, E. Meffre, K. Kayentao, A. Ongoïba, B. Traoré, and S. K. Pierce. 2015. The V gene repertoires of classical and atypical memory B cells in malaria-susceptible West African children. *J. Immunol.* 194: 929–939.
20. Portugal, S., C. M. Tipton, H. Sohn, Y. Kone, J. Wang, S. Li, J. Skinner, K. Virtaneva, D. E. Sturdevant, S. F. Porcella, et al. 2015. Malaria-associated atypical memory B cells exhibit markedly reduced B cell receptor signaling and effector function. *ELife* 8: 4.
21. Yates, J. L., R. Racine, K. M. McBride, and G. M. Winslow. 2013. T cell-dependent IgM memory B cells generated during bacterial infection are required for IgG responses to antigen challenge. *J. Immunol.* 191: 1240–1249.
22. Wang, Z., M. Raifu, M. Howard, L. Smith, D. Hansen, R. Goldsby, and D. Ratner. 2000. Universal PCR amplification of mouse immunoglobulin gene variable regions: the design of degenerate primers and an assessment of the effect of DNA polymerase 3′ to 5′ exonuclease activity. *J. Immunol. Methods* 233: 167–177.
23. Whittle, J. R., A. K. Wheatley, L. Wu, D. Lingwood, M. Kanekiyo, S. S. Ma, S. R. Narpala, H. M. Yassine, G. M. Frank, J. W. Yewdell, et al. 2014. Flow cytometry reveals that H5N1 vaccination elicits cross-reactive stem-directed antibodies from multiple Ig heavy-chain lineages. *J. Virol.* 88: 4047–4057.
24. Zanotti, K. J., R. W. Maul, D. P. Castiblanco, W. Yang, Y. J. Choi, J. T. Fox, K. Myung, H. Saribasak, and P. J. Gearhart. 2015. ATAD5 deficiency decreases B cell division and Igh recombination. *J. Immunol.* 194: 35–42.
25. Scholz, J. L., J. E. Crowley, M. M. Tomayko, N. Steinel, P. J. O'Neill, W. J. Quinn, III, R. Goenka, J. P. Miller, Y. H. Cho, V. Long, et al. 2008. BLyS inhibition eliminates primary B cells but leaves natural and acquired humoral immunity intact. *Proc. Natl. Acad. Sci. USA* 105: 15517–15522.
26. Cancro, M. P., W. Gerhard, and N. R. Klinman. 1978. The diversity of the influenza-specific primary B-cell repertoire in BALB/c mice. *J. Exp. Med.* 147: 776–787.
27. Naradikian, M. S., Y. Hao, and M. P. Cancro. 2016. Age-associated B cells: key mediators of both protective and autoreactive humoral responses. *Immunol. Rev.* 269: 118–129.
28. Viale, A. C., J. A. Chies, F. Huetz, E. Malenchere, M. Weksler, A. A. Freitas, and A. Coutinho. 1994. VH-gene family dominance in ageing mice. *Scand. J. Immunol.* 39: 184–188.
29. Ben-Yehuda, A., P. Szabo, J. LeMaoult, J. S. Manavalan, and M. E. Weksler. 1998. Increased VH 11 and VH Q52 gene use by splenic B cells in old mice associated with oligoclonal expansions of CD5+ B cells. *Mech. Ageing Dev.* 103: 111–121.
30. Riley, S. C., B. G. Froscher, P. J. Linton, D. Zharhary, K. Marcu, and N. R. Klinman. 1989. Altered VH gene segment utilization in the response to phosphorylcholine by aged mice. *J. Immunol.* 143: 3798–3805.
31. LeMaoult, J., S. Delassus, R. Dyall, J. Nikolić-Zugić, P. Kourilsky, and M. E. Weksler. 1997. Clonal expansions of B lymphocytes in old mice. *J. Immunol.* 159: 3866–3874.
32. Wardemann, H., S. Yurasov, A. Schaefer, J. W. Young, E. Meffre, and M. C. Nussenzweig. 2003. Predominant autoantibody production by early human B cell precursors. *Science* 301: 1374–1377.
33. Lebecque, S. G., and P. J. Gearhart. 1990. Boundaries of somatic mutation in rearranged immunoglobulin genes: 5′ boundary is near the promoter, and 3′ boundary is approximately 1 kb from V(D)J gene. *J. Exp. Med.* 172: 1717–1727.
34. Goenka, R., A. H. Matthews, B. Zhang, P. J. O'Neill, J. L. Scholz, T. S. Migone, W. J. Leonard, W. Stohl, U. Hershberg, and M. P. Cancro. 2014. Local BLyS production by T follicular cells mediates retention of high affinity B cells during affinity maturation. *J. Exp. Med.* 211: 45–56.
35. Voigt, I., S. A. Camacho, B. A. de Boer, M. Lipp, R. Förster, and C. Berek. 2000. CXCR5-deficient mice develop functional germinal centers in the splenic T cell zone. *Eur. J. Immunol.* 30: 560–567.
36. Di Niro, R., S. J. Lee, J. A. Vander Heiden, R. A. Elsner, N. Trivedi, J. M. Bannock, N. T. Gupta, S. H. Kleinstein, F. Vigneault, T. J. Gilbert, et al. 2015. *Salmonella* infection drives promiscuous B cell activation followed by extrafollicular affinity maturation. *Immunity* 43: 120–131.
37. Pape, K. A., J. J. Taylor, R. W. Maul, P. J. Gearhart, and M. K. Jenkins. 2011. Different B cell populations mediate early and late memory during an endogenous immune response. *Science* 331: 1203–1207.
38. Weisel, F. J., G. V. Zuccarino-Catania, M. Chikina, and M. J. Shlomchik. 2016. A temporal switch in the germinal center determines differential output of memory B and plasma cells. *Immunity* 44: 116–130.
39. Naradikian, M. S., A. Myles, D. P. Beiting, K. J. Roberts, L. Dawson, R. S. Herati, B. Bengsch, S. L. Linderman, E. Stelekati, R. Spolski, et al. 2016. Cutting edge: IL-4, IL-21, and IFN-γ interact to govern T-bet and CD11c expression in TLR-activated B cells. *J. Immunol.* 197: 1023–1028.

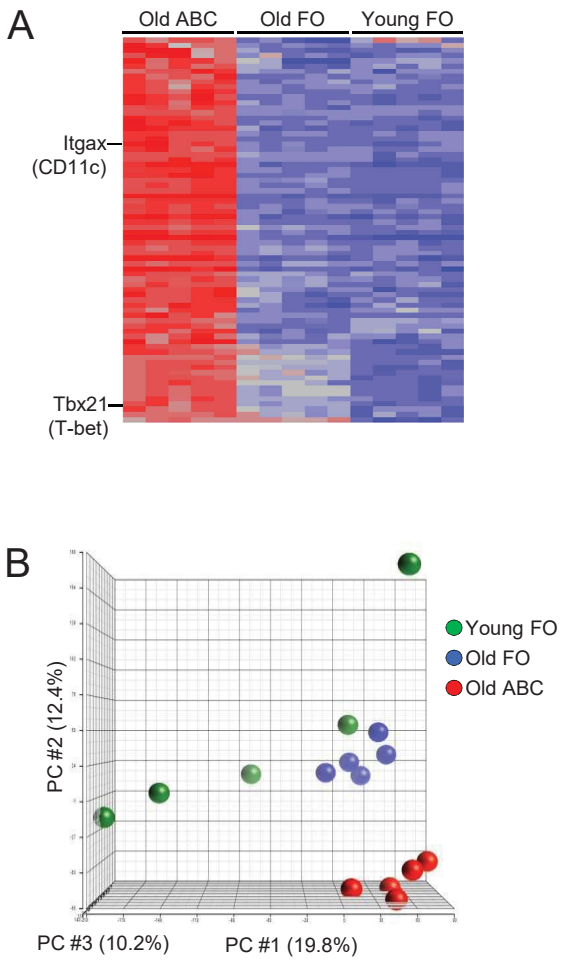

FIGURE S1. ABCs display a distinct gene expression profile.
(A) Heat map showing relative expression levels of transcripts that are at least 5-fold higher (red) in old ABCs compared to old FO B cells or young FO cells (blue). Gene names are provided in Table S1. (**B**) Principal component analysis of all genes expressed in young FO, old FO, and old ABC, sorted from 5 young and 5 old mice. The first, second, and third components account for 42.4% of the variance in the data matrix.

Table S1. List of transcripts ≥ 5-fold higher in old ABC compared to old FO (shown in Fig. S1A)

Gene symbol	Gene name
Rgs1	regulator of G-protein signaling 1
Ccl19	chemokine (C-C motif) ligand 19
Ctla4	cytotoxic T-lymphocyte-associated protein 4
Il10	interleukin 10
Fam46c	family with sequence similarity 46, member C
Id2	inhibitor of DNA binding 2
S1pr3	sphingosine-1-phosphate receptor 3
Sh2d1b1	SH2 domain containing 1B1
Abcb1b	ATP-binding cassette, sub-family B (MDR/TAP), member 1B
Ramp3	receptor (calcitonin) activity modifying protein 3
Nrp2	neuropilin 2
Parm1	prostate androgen-regulated mucin-like protein 1
Havcr1	hepatitis A virus cellular receptor 1
Anxa2	Mouse annexin
Rbm47	RNA binding motif protein 47
Chn2	chimerin 2
Nt5e	5' nucleotidase, ecto
Il2rb	interleukin 2 receptor, beta chain
Art3	ADP-ribosyltransferase 3
4930506M07Rik	shootin 1
Itgax	integrin alpha X (CD11c)
Cxcl10	chemokine (C-X-C motif) ligand 10
Ptpn22	protein tyrosine phosphatase, non-receptor type 22 (lymphoid)
Cd300lf	CD300 molecule like family member F
Gm5486	M. musculus predicted gene 5486
Sirpa	signal-regulatory protein alpha
Zbtb32	zinc finger and BTB domain containing 32
Cd80	CD80 antigen
Gm1965	M. musculus predicted gene 1965
Cd80	CD80 antigen (RIKEN library)
Gpr55	G protein-coupled receptor 55
Cdk14	cyclin-dependent kinase 14
Lcp2	lymphocyte cytosolic protein 2
Emr1	adhesion G protein-coupled receptor E1 (Adgre1)
Itgb1	integrin beta 1 (fibronectin receptor beta)
Zeb2	zinc finger E-box binding homeobox 2
Bmpr1a	bone morphogenetic protein receptor, type 1A
Fgl2	fibrinogen-like protein 2
Lilrb4	leukocyte immunoglobulin-like receptor, subfamily B, member 4A
Zbtb20	zinc finger and BTB domain containing 20
Rcn3	reticulocalbin 3, EF-hand calcium binding domain
Fah	fumarylacetoacetate hydrolase
Zbtb20	zinc finger and BTB domain containing 20
Fcer1g	Fc receptor, IgE, high affinity I, gamma polypeptide
Itm2c	integral membrane protein 2C
Ptpn14	protein tyrosine phosphatase, non-receptor type 14
Grk5	G protein-coupled receptor kinase 5
Zc3h12c	zinc finger CCCH type containing 12C
Gp49a	leukocyte immunoglobulin-like receptor, subfamily B, member 4B
Bhlhe41	basic helix-loop-helix family, member e41
Apoe	apolipoprotein E
Itgam	integrin alpha M
Ahnak	AHNAK nucleoprotein (desmoyokin)
Cd3g	CD3 antigen, gamma polypeptide
Lgals1	lectin, galactose binding, soluble 1
AK081116	Hypothetical Gag gene protein p24
Apoc2	apolipoprotein C-II
Plscr1	phospholipid scramblase 1
LOC100041877	nuclear body protein SP140-like
Naip5	NLR family, apoptosis inhibitory protein 5
Fcrl5	Fc receptor-like 5
Trabd2b	TraB domain containing 2B
Naip6	NLR family, apoptosis inhibitory protein 6
Atxn1	ataxin 1
Gm7609	predicted pseudogene 7609 (Gm7609)
Ackr2	atypical chemokine receptor 2
Tbx21	T-box 21 (T-bet)
Fas	Fas (TNF receptor superfamily member 6)
Mpeg1	macrophage expressed gene 1
G530011O06Rik	RIKEN cDNA G530011O06 gene

Gene names are from the NCBI Nucleotide or Ensembl databases. Transcripts are listed in order from top to bottom of Fig. S1A. Duplicates either map to different clones of the same gene (CD80, Zbtb20) or are repeats of the same RefSeq (Gm1965, Gm7609, Plscr1, Zc3h12c). This dataset is available through the NCBI GEO repository (dataset GSE81650).